CHAPTER 3

3 EXTENSION OF THE MODEL TO INCLUDE A FORCING FUNCTION FOR STRUCTURAL STORAGE

Structural storage is by definition an indoor climate control system where the heat storage capability of the massive structures of the building are actively utilized. For instance, if the outdoor air temperature is lower than the bulk structure temperature during the night, this cool night air may be used to cool the structure. During the hot hours the structure is then allowed to absorb some of the excess heat of the interior air. The functioning and application of this type of system is further discussed in §3.1. It is the objective of this chapter to examine the modelling of this type of system and to extend the model of Mathews and Richards to cater for such systems.

3.1 Introduction

It is by now fairly well known (see references [1] and [2]) that the highveld climate, with large diurnal temperature swings, admits the possibility of conditioning of buildings without mechanical refrigeration. In addition, since a mechanical refrigeration system is complex, expensive to install and in constant need of maintenance, a considerably economic advantage can be realized even if just the cooling capacity of an active indoor climate control system can be reduced. One method for achieving these objectives is too use cool night time air to remove heat from the massive structure of the building when the building is unoccupied. During the hot, occupied hours the temperature of the interior air is then reduced by the absorption of excess heat into the pre–cooled structure. This concept is known as structural storage since it actively utilizes the heat storage capability of the building. It is obviously only applicable to buildings which are relatively massive and which are unoccupied during the night i.e. office blocks. To be successful, structural storage systems require careful thermal design of the passive thermal response of the building and close co–operation between architect and engineer. According to an analysis by

van Aarle and Herman [1], structural storage systems are successful if the thermal design of the building takes into account the following criteria:

"(a) Fenestration

Minimum possible, and shaded on the outside from solar penetration, not only direct, but also sky– and reflected radiation.

double glazing is not necessary for summer (maybe should be considered for winter.) Higher heat loss during the night is beneficial and just about offsets higher heat gain during the day.

(b) Walls

Heavy structure to provide storage mass. Insulation not a necessity for summer.

(c) Roof

Heavy structure. Should always be insulated. Insulation to be on outside.

(d) Lighting

Efficient lighting can now be provided at not more than 10–15 W/m^2.

(e) People density

The number of people in a room can obviously not be controlled.

(f) Equipment load

Normal office equipment can easily be handled. Typing pool type loads in the order of 40 W/m^2 require an increased air quantity."

Van Aarle and Herman also point out that the highveld climate, with it's relatively large diurnal temperature variations, are ideally suited for these systems. But if structural cooling is to find general acceptance in South Africa, an appropriate design tool is required for predicting the performance of buildings containing these systems. From the considerations given above it is clear that such a tool must be dual purpose. It must be

able to guide the architect in the initial design stages of the building; so that a building design with optimum thermal properties results. In addition, it must be an aid to the consulting engineer for designing the conditioning system. The simple model and accompanying computer program of Mathews and Richards, as discussed in previous sections of this thesis, will be extremely suitable as an aid for designing buildings with structural storage, if it is extended to include the possibility of heat extraction from the structure.

In this thesis the fundamental principles behind structural storage is briefly dealt with. A simple model, applicable to most types of structural storage systems, is derived. The implementation of this model is accomplished in a manner that the data input requirements are modest and reasonable. The operator must specify which surfaces are subject to structural storage and what the heat exchange coefficients of these surfaces are. In addition, the operator can either specify the use of external air for storage purposes, or alternatively, pre–cooled air such as would be obtained from an evaporative cooling system. The inclusion of these extra capabilities is done without jeopardizing the speed and ease of use of the simulation of the thermal response.

In this thesis we are not so much concerned with the merits of structural storage. The aim is simple; to be able to simulate the effect of structural cooling on the thermal performance of buildings, in a sufficiently general way, that various cooling systems may be evaluated. With regard to the use of the model and computer program, it is recognized that the building designer will only be able to make use of the program if the data input and user interface is sufficiently simple and logical. If a very detailed specification of the structure is required, at a stage when the structure is still largely undefined, the program will have no use for architects. It seems appropriate to simplify to the extreme and to sacrifice some accuracy of prediction in order to have a useful architectural tool. It must be

remembered that the architect will mainly utilize the program to compare the relative merits of different designs.

On the other hand, if the program is to be useful for engineers designing the conditioning systems which control the indoor climate, the method must be sufficiently accurate and contain enough detail for valid design optimization. By balancing these two – somewhat contradictory – requirements of architect and engineer, we believe a very useful and generally applicable program results which can be used with confidence by all. Furthermore, the combination of passive building response and conditioning design in one program, will hopefully facilitate a design methodology, where these two aspects are treated in an integrated manner and the optimum design is realized. (At least in so far as the passive thermal response is concerned). Our final aim is to be able to evaluate various conditioning systems and building designs, and to optimize these, in a program which assimilates building and conditioning unit in one total thermal system.

3.2 The Principles of Structural Storage

In it's widest sense the term structural storage can be applied to any conditioning system which, instead of directly attempting to affect the interior air–temperature, does so indirectly by attempting to influence the amount of heat stored in the massive structure. Strictly speaking, such systems include extraction or addition of heat from and to the structure by any means, e.g. by means of a fluid being forced through channels inside the structure. In practice the method employed is normally to force cool air to flow across the surfaces of the structure, a method which requires very little extra complications in the structural design of the building. In all these systems the rate of heat transfer between fluid and structure is the primary design characteristic. It is, as usual, expressed in terms of a

heat transfer coefficient. In this section we briefly investigate the models for convective heat transfer from the literature[1]. We restrict ourselves to forced convection between a surface and a fluid flowing across the surface.

If the surface is flat and isothermal, and, a constant heat flux exists between the surface and the fluid, and furthermore, the air flow is laminar, Holman [3] indicates that the heat transfer between surface and fluid is given by:

$$\overline{T_w - T_\infty} = \frac{q_w \cdot L/k \cdot A}{0.6795 \cdot Re^{1/2} \cdot Pr^{1/3}}. \tag{3.1}$$

In this equation $\overline{T_w - T_\infty}$ is the mean temperature difference between the surface and the free–flowing fluid, L is a typical contact length [m], k is the conductivity of the fluid [kW/m·K], A is the area across which heat transfer takes place [m^2], Re is the Reynolds number, defined in terms of the contact length:

$$Re = \rho \cdot u_\infty \cdot L/\mu \tag{3.2}$$

with ρ specific density [kg/m^3], u_∞ free stream velocity [m/s] and μ the dynamic viscosity [kg/s·m]. Pr is the Prandtl number given by:

$$Pr = c_p \cdot \mu/k \tag{3.3}$$

with c_p the specific heat capacity of the fluid [kJ/kg·K]. This equation can obviously be written in the form of a generalized Newton's law of cooling:

$$q = \bar{h}_w \cdot A \cdot \overline{(T_w - T_\infty)} \tag{3.4}$$

with the appropriate definition of the mean convective heat transfer coefficient $\bar{h}_w$. Although equations (3.1) to (3.4) can often be used to obtain a preliminary estimate of the order of magnitude of the heat transfer coefficient it (and other similar equations) is not sufficiently accurate for design purposes. For a more accurate value it is essential to build a mock–up and to investigate the matter experimentally.

[1]These results are well known and are included here for the sake of completeness and to aid newcomers to the topic.

In general, Newton's law of cooling can only be applied locally to the interface in the form:

$$q(x) = h_w(x) \cdot [T_w(x) - T_\infty]. \tag{3.5}$$

with x the distance measured in the direction of the flow from the first point of contact between surface and fluid. (Actually this is a definition of the local heat transfer coefficient per unit area.) The heat transfer coefficient depends upon the details of the thermal boundary layer and hence on the details of the flow and construction. In the theories of boundary layer heat transfer, it is convenient to work with non–dimensional groups and the local heat transfer coefficient is usually given in terms of the non–dimensional Nusselt number given by:

$$Nu_x = \frac{h_w x}{k} \tag{3.6}$$

with x a spatial dimension in the direction of the flow. The Nusselt number is a strong function of the flow details (laminar, turbulent, surface friction etc.), and also of distance along the direction of the flow. To determine the Nusselt number it is thus necessary to know the exact geometry and also the velocity profile of the flow. However, many simplified relations are available in the literature which correlates total heat transfer in terms of the average Nusselt number $\bar{Nu}$. Holman [3] gives the following empirical formula:

$$\bar{Nu} = C \cdot Re^m \cdot Pr^n \tag{3.7}$$

with C, n and m empirical constants to be determined from the experimental data for each type of structure. In (3.7) the Nusselt number is defined with reference to the total length of the surface in contact with the fluid, in the direction of the flow.

Doyle and Johannsen [2] thoroughly investigated the thermal heat transfer coefficient for a structure consisting of a 100 mm thick concrete slab in a plenum. Different air velocities were used with continuous monitoring of the slab and air temperatures. They found that the actual heat transfer coefficients at the surface of the slab ranged from 9 to 18 $W/m^2 \cdot K$, for air velocities between 0,46 and 2 m/s. The theoretical values were 2,3 to 5,9 $W/m^2 \cdot K$. They ascribed this discrepancy to the turbulent nature of the air and to radiative heat exchange. Nonetheless, they found good agreement with the heat transfer coefficient derived by exact numerical modelling of the heat exchange mechanism. From these results it appears unlikely that the simple theoretical or empirical relationships above will be of much practical value, unless values for the coefficients in (3.7) is determined experimentally. Alternatively, one can also use extensive computer modelling and simulation of the exact structural geometry and air flow to obtain better estimates of the heat transfer coefficients.

A standard reference, ASHRAE Handbook [4], presents the following simplified equations for forced convection between a vertical plane surface and air:

For wind speeds V in the range $5 < V < 30$ m/s:

$$h = 7.2 \cdot V^{0.78}. \tag{3.8}$$

For wind speeds $V < 5$ m/s:

$$h = 5.6 + 18.6 \cdot V \tag{3.9}$$

These equations do not correspond with equations from other authors, e.g. (3.1), where the wind speed normally enters with a half power law. They also disagree with the measured coefficients from [2] given in the previous paragraph[2].

[2]Actually (3.9) yields highly unrealistic values, e.g. with $V = 4$ m/s, h is 80 $W/m^2 \cdot K$, a very dubious value. The equation is probably in error and the original reference must be consulted.

One is forced to conclude that the literature is of little benefit with regard to the provision of accurate values for the heat transfer coefficients, and that good engineering judgment will be required. There is no valid, sufficiently general relation for determining the value of the heat transfer coefficient. Each particular case will require individual attention. It is hopeless to try to include in a model all the various geometrical structures and flow conditions which may be encountered in practice. Such an approach will furthermore seriously inhibit the creativeness of the designer and reduce the scope available to the engineer. It will be sufficient to assume that Newton's law of cooling is applicable in a general sense and to leave the problem of deciding what heat transfer coefficient to use, to the judgment of the designer. It will be necessary to give some guidance in this respect to the architect, probably in the form of a suggestion of what coefficient to use for certain types of structures, based on actual measurements. The air–conditioning engineer will obviously need to investigate the dependence of the heat transfer coefficient on the volume flow and other parameters, to optimize the design. This facility can be included in the program by programming equation (3.7) so that the engineer can specify experimental values for C, n and m and then investigate the consequences when e.g. the flow velocity or other parameters are varied. The architect need not even be aware of this facility in the program since he simply picks a heat transfer coefficient (possibly guided by a help screen) as a design goal for the engineer or from past experience. Obviously architect and engineer should closely co–operate.

To summarize this section we observe that it will be convenient and sufficient to assume Newton's law of cooling valid for the mean temperature difference between wall and fluid, and to include all the structural and flow details in the value assigned to the heat transfer coefficient.

3.3 The Equivalent Electrical Circuit with Structural Storage

In this section a simple model for structural storage, based on Newton's law of cooling, is presented and it is shown that this model can be easily incorporated in the thermo–flow network of Mathews and Richards; discussed in chapter 2.

3.3.1 The Definition of the Heat Transfer Coefficient

It was indicated in §3.2 that Newton's law of cooling, will be assumed generally valid for structural storage heat transfer. In (3.4) T_w is the surface temperature of the wall, a quantity which is not represented in the simplified network of figure 2.1. In the thermal model of Mathews and Richards only one temperature, T_c, is used which represents the bulk storage temperature. The temperature at the wall surface will normally differ considerably from this bulk temperature, since a thermal gradient exists across the wall. The problem of correct identification of the wall surface temperature in the model of Mathews and Richards is one of the main reasons which led to the proposal of a somewhat more refined model in §2.6. Nevertheless, to keep the network simple, and to stick to the model of Mathews and Richards, the convective surface temperature T_w will be identified with T_c in figure 2.1. In effect this implies that the heat transfer coefficient must be defined in the following manner:

$$h_{sc} = \frac{\overline{T_{sc} - T_c}}{q \cdot A} \tag{3.10}$$

where T_{sc} is the free–stream temperature of the fluid and q is the heat flux, and the bar designates the average difference between bulk structure temperature and free–stream fluid temperature. This definition of the heat transfer coefficient differs significantly from the normal definition as used in (3.4), so that it will not be possible, strictly speaking, to use the transfer coefficients from the literature in our model. This disadvantage can be overcome by using the more refined model of figure 2.21, but for the present discussion, we limit ourselves to the model of Mathews and Richards.

Note that the above definition of h_w will correspond with those in the literature when the temperature of the structure is uniform. In practice, uncertainties in the flow rates, fluid temperature, surface finish etc. probably overshadow this uncertainty caused by the actual differences in definition. The main point is that in future, empirical research aimed at determining structural storage heat transfer coefficients, to be used with this thermal model, should preferably use the definition (3.10). Also, when transfer coefficients are taken from the literature, the differences in definitions must be recognized and taken account of.

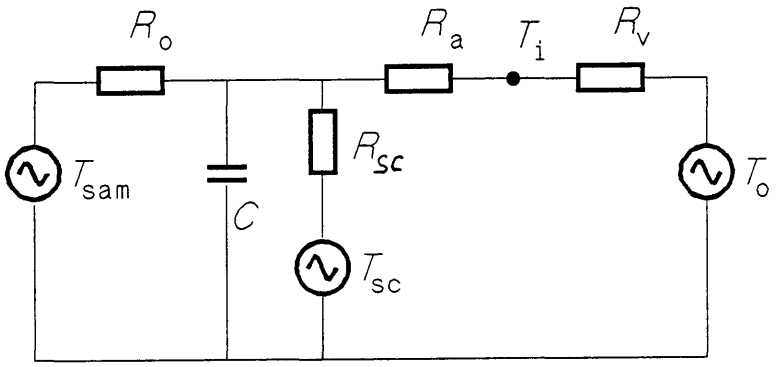

FIGURE 3.1 The model of figure 2.1 extended to include structural storage. T_{sc} is the additional forcing function which operates on the structure, through the time dependent resistor R_{sc}.

The definition according to equation (3.10) is easy to incorporate in the network of figure 2.1. The heat transfer coefficient can be modelled as a conductance connecting the T_c node with a new independent source, the structural storage source T_{sc}, which represents the free–stream temperature of the fluid. In many practical systems the outside air will be used as cooling fluid so that T_{sc} will be equal to the outside air–temperature. If pre–cooled air is used as fluid, T_{sc} must equal the temperature of the

pre–cooled air. The new network appears in figure 3.1 where we have defined

$$q = \frac{T_{sc} - T_c}{R_{sc}} \tag{3.11}$$

R_{sc} represents the inverse of the combined heat transfer coefficients of all the surfaces. It's value will approach infinity when the heat transfer coefficients of all the surfaces are zero. If the heat transfer coefficients are very large R_{sc} will vanish, indicating that the temperature of the structure must equal that of the outside air.

3.3.2 The Combined Heat Transfer Coefficient

In figure 3.1 we have blandly used one resistance and one source to model the combined effect of the various surfaces subject to structural storage. This requires some further explanation. The thermal network contains a single heat store, the capacitance in figure 3.1, which represents the combined effect of all the massive elements of the structure. The assumption underlying this network is that all the massive elements of the building, which contribute to the storage of heat, are at the same instantaneous temperature[3]. The assumption is founded on the premise that the interior surfaces of the walls are all approximately at the same temperature, due to radiative and convective exchange of heat in the interior. Furthermore, it is assumed that the bulk temperature of all the massive structures is fairly uniform. An obvious objection which might be raised, is that those surfaces which are subjected to cooling will have lower temperatures than the other uncooled structures. This objection is well justified, but is to some extend countered by the assumption that the interior surfaces will, via radiation, tend to equalize the temperatures. The advantage of the network of figure 3.1 is it's clear physical interpretation, and from measurements it appears that the essential features of the thermo–flow problem, that is, the mean rate of heat energy inflow minus outflow to the building structure, is adequately modelled.

[3]For a discussion of the assumptions on which the network of figure 3.1 is based refer to chapter 2 of this thesis.

Assuming then that all the surfaces are being cooled with air at the same bulk temperature T_{sc}, the combined effect is given by adding the contribution of each surface to the total heat flow, so that the active heat stored in the structure is correctly represented. This is fully in accordance with the philosophy of the simplified network as discussed in chapter 2. That is, the capacitor in the network is not the physical capacitance but represents the active heat stored in the massive structure. The total effect of all the surfaces subject to structural cooling is conveniently obtained by adding the individual heat transfer coefficients together. Normally the coefficients would be given in terms of a unit of area so that the total heat transfer coefficient of all n surfaces is:

$$h_{sc} = 1/R_{sc} = A_1 \cdot h_{s1} + A_2 \cdot h_{s2} + ... + A_n \cdot h_{sn} \qquad (3.12)$$

where A_i is the area and h_{si} the structural storage heat transfer coefficient of surface number i.

3.4 Implementation

The solution of the network of figure 3.1 is very straightforward and can be obtained in exactly the same form as the solution of the network of figure 2.1. The solution of the network of Mathews and Richards is discussed in chapter 5, where it is shown that all the forcing function can be combined in two effective forcing functions, T_x and T_y of (5.24). The solution of the circuit of figure 3.1 is given by redefining T_y in (5.24) to include the new independent temperature T_{sc}:

$$T_y = \frac{Q_r \cdot R_o \cdot R_{sc} + T_{sa} \cdot R_{sc} + T_{sc} \cdot R_o}{R_o + R_{sc}} \qquad (3.13)$$

and to define a new resistance R_y, taking the place of R_o in the solution:

$$R_y = \frac{R_o \cdot R_{sc}}{R_o + R_{sc}}. \qquad (3.14)$$

With this new definition of T_y, and by substituting R_y for R_0, the solution proceeds as before via equations (5.23) to (5.34).

Very little programming changes are required to include the extra calculations. Of more importance is the additional input data required to specify the heat transfer coefficient of each surface which are subjected to structural cooling, the temperature of the cooling air and the daily cycle of structural storage. By daily cycle we mean more than just switching the system on and off. Some practical systems use the structural storage system to provide ventilation during the day [2]. In this case, the air is diffused into the zones after it's contact with the structure. This setup provides for both ventilation and structural cooling with a single system. In these systems the daytime flow–rate is usually much lower than during the night. In the next section we examine the modelling of such systems.

3.4.1 The Daily Cycle

Specification of the daily cycle presents something of a problem. In §3.1 it was pointed out that the dependency of the convective heat transfer on the velocity of the cooling air depends on specific details, such as the level of turbulence and the geometry of the flow. A generally valid equation, which gives the heat transfer coefficient in terms of the fluid velocity, does not exist. Consequently, it appears impracticable to incorporate a rule which determines the heat transfer from specified hourly volume flows or speeds, although this seems the most natural method. This problem may be circumvented by adjusting the value of the heat transfer coefficient hourly to yield the correct heat flux. A straightforward way of accomplishing this is to specify percentage cooling on an hourly basis. This will plainly indicate the percentage heat flow on a linear scale, with 100 % cooling equal to the maximum heat flux. To demonstrate: if a total area of 10 m^2, with heat transfer coefficient 20 $W/m^2 \cdot K$ is subject to 50% cooling, with a 10 ^oC temperature difference between structure and cooling air, the total heat flux will be 20 $[W/m^2 \cdot K] \cdot 10\ [m^2] \cdot 50\% \cdot 10\ [^oC] = 1\ [kW]$. This method is not fully satisfactory, but until a proper, acceptable law is available for the

heat transfer coefficient under diverse circumstances, it will have to suffice. If the flow rate is reduced during the day, the designer must determine the heat transfer rate with the lower flow speed as a percentage of the heat transfer rate at maximum speed. These percentages are then specified hourly. It is assumed that all the surfaces are similarly affected and the percentage value will have the effect of reducing the total heat flux to the prescribed percentage of the maximum.

The enhanced model of figure 3.1, which incorporates structural storage, was implemented in the program. A listing of the relevant sections of the program is provided on the floppy diskette included in the back–cover of this thesis.

3.4.2 Verification of the Model

The verification of the model is straightforward. Since an empirical variable – the heat transfer coefficient – is used, the accuracy of the prediction will be determined solely by the accuracy of the specified heat transfer coefficient. In fact, the best way for determining the heat transfer coefficient is to work backwards, and to select a heat transfer coefficient which gives the best prediction in relation to measurements, in each particular case. This procedure is demonstrated in the next section. The implementation of the thermal model, with structural storage included, can be further verified by examining the behavior of the program in limiting cases. When no structural cooling takes place, i.e. when the heat transfer coefficients for all the surfaces are 0, the program should yield the same results as previous versions which did not incorporate structural cooling. Furthermore, when the heat transfer rate is very large, the interior temperature should be close to the temperature of the outside air[4]. Figure 3.2 presents demonstrative results where all the surfaces of a building are subjected to cooling at a large rate. It can be seen that the interior

[4]If it is assumed that outside air is used as cooling fluid. A more accurate statement is: the temperature should approach the free–stream temperature of the cooling fluid.

temperature closely approximates the temperature of the exterior air, which was used to cool the structure.

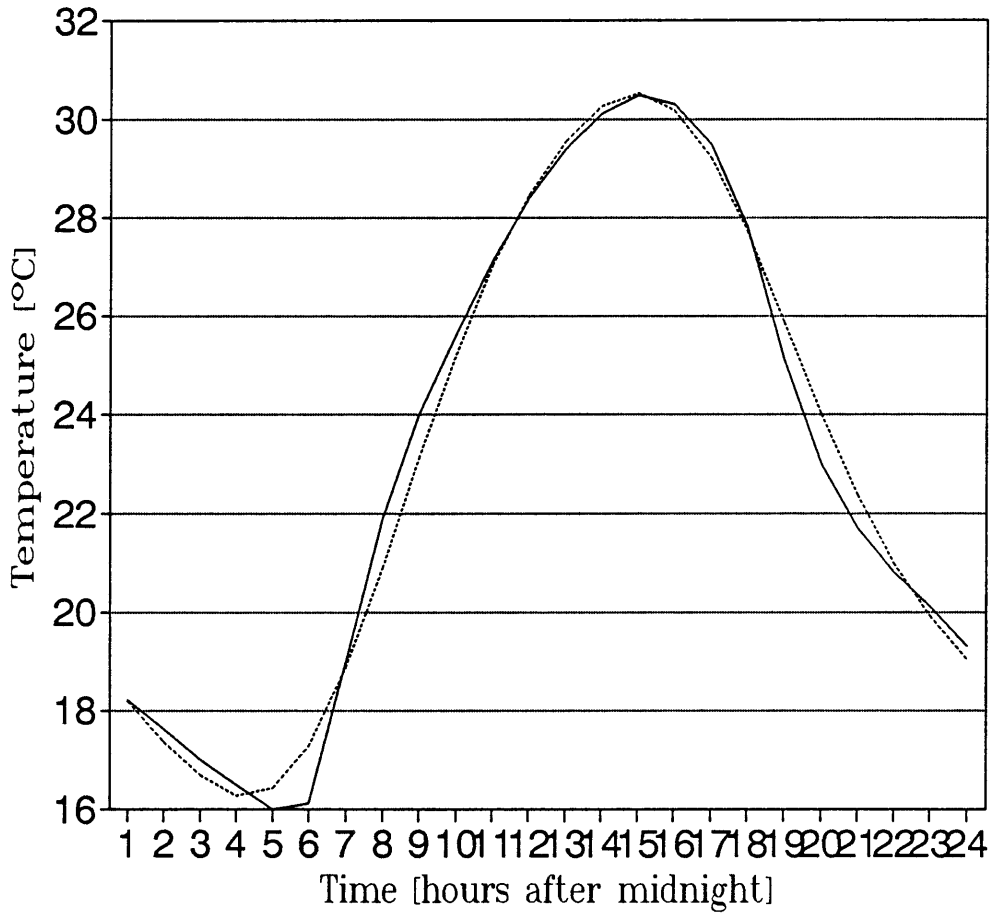

FIGURE 3.2 Interior temperatures in a building with all walls cooled at a large rate. The interior temperature should approach the exterior air–temperature.

The program seems to be behaving quite well when the hourly rate of cooling is varied. Problems do arise though when the heat transfer rate is excessively high (non physical rates exceeding 50 $W/m^2 \cdot K$) and large

hourly variations are specified. In this case the sudden, extreme changes in heat transfer rate causes serious numerical errors in the answer. This problem can be eliminated by limiting the heat transfer coefficients to the range 0 to 50 $W/m^2 \cdot K$.

3.4.3 Measured Heat Transfer Coefficients in a Test Hut[5]

The model can also be verified by comparison of measured results with predicted results, provided the exact heat transfer coefficient is known. Unfortunately, as discussed before, the definition of the heat transfer coefficient in (3.10) differs from the usual definition in the literature, so that theoretical or empirical predictions can not be used. In any case, there is some doubt about the validity of the usual equations in the literature [2], as indicated in §3.2. To investigate this issue an experiment was set up in a test hut, which was equipped with air ducts in the concrete floor. For a complete description of the experiment see [5]. Pre–cooled air was blown through the ducts during the hours 18h00 to 06h00. The heat transfer rate from the slab to the air in the ducts was determined iteratively by guessing values until the predicted interior temperature of the thermal model closely resembled the measured interior temperature. The value so obtained was $\underline{h}_w \approx 7$ $W/m^2 \cdot K$. This 'measured' coefficient was compared with the value obtained from the empirical correlation of Ditties and Boelter [3], which was applicable to the flow. The values agreed very well. This result must be viewed in contrast with the results reported in [2], where it was found that the usual equations for convection coefficients are insufficient. We come to the conclusion that each case will merit individual attention, and that the correct heat transfer coefficient for a specific design must be experimentally determined.

3.5 Some Typical Results

The main aim of structural storage is to reduce the daytime temperature

[5]Acknowledgment is due to JH Grobler who carried out the experiments in the test hut, described in §3.4.3.

by cooling the structure with cool night air. It should be possible, from analysis of the network of figure 3.2, to study the economics and applicability of structural storage in various climates and seasons. Since the brief of this study is the inclusion of structural storage in the thermal model, it is not the intention to discuss the relative merit of such a system here. These issues are, to some extend, treated in references [1,2 and 6] which all come to the conclusion, that, provided care is taken in the design of the building and the conditioning system, real energy savings are possible on the highveld.

In this section we present some illustrations of the influence of night time cooling of the structure on the interior temperature of buildings, with the aim to demonstrate the utility and application of the new modified program.

3.5.1 A massive structure

Figure 3.3 presents the influence of structural storage on a massive structure, an office block with 300 mm poured concrete floors. A typical centre floor north office in this block is simulated. The office possesses a north wall consisting of 150 mm poured concrete. The other walls are of light construction. In figure 3.3 graphs of the outside air and the inside air with various heat transfer coefficients are shown. It was assumed that the cool night air is used between 21h00 and 06h00 to cool the intermediate floors. Heat transfer coefficients of 0, 5, 10, 20 and 30 $W/m^2{}^oC$ were used. (Note that these values refer to the office being simulated. Since there are two offices bordering each intermediate floor, the one above and the one below, the actual heat transfer rate from the slab must be twice these values.)

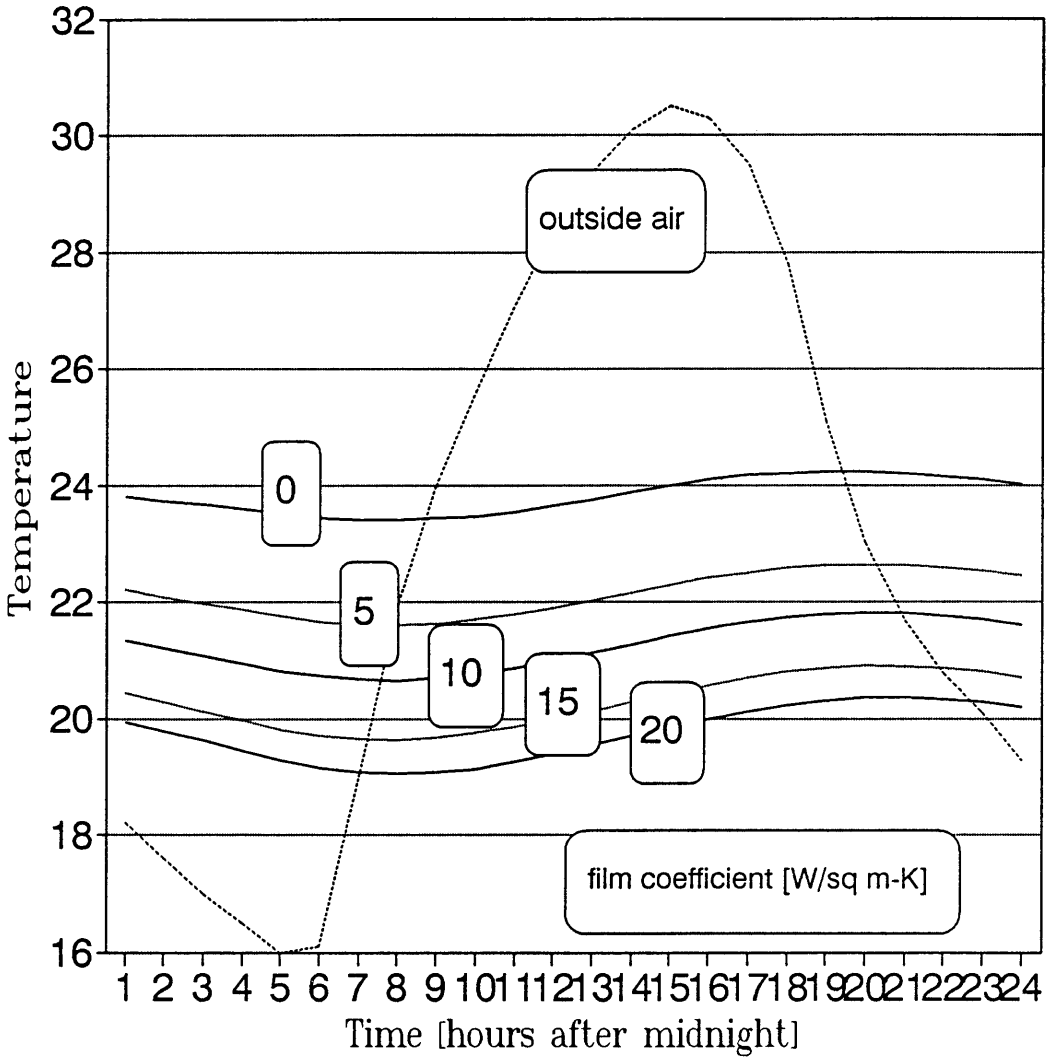

FIGURE 3.3 Night cooling of a massive structure (office).

The structural storage clearly has a pronounced effect on the interior temperature. With a heat transfer coefficient of only 5 $W/m^2{}^oC$ the interior temperature is lowered by nearly 2 ^oC. The graphs indicate that increases in the value of the heat transfer coefficient yields diminishing

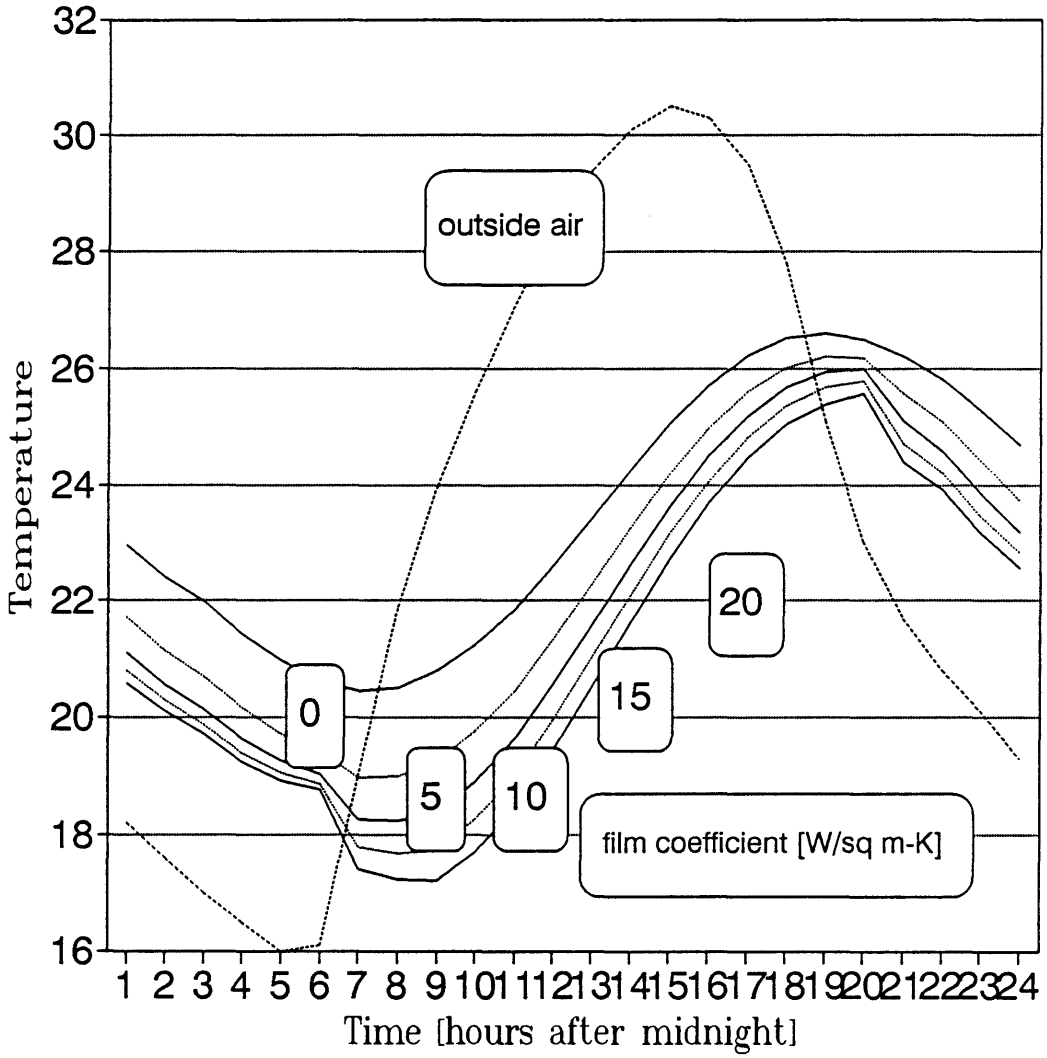

FIGURE 3.4 Night cooling of a lightweight structure.

returns. This is easily explained by noting that the slab temperature can not be lowered below the air temperature. A large heat transfer coefficient would bring the slab temperature to the outside air temperature and further increases in the coefficient will not yield any returns. It follows that

an optimum (in the economic sense) heat transfer coefficient must exist where the maximum effect is obtained for the lowest expense.

3.5.2 A lightweight structure

Figure 3.4 shows similar results for a relatively lightweight structure; a test hut in Israel with a pressed asbestos cement roof with well insulated ceiling, walls of pressed asbestos cement insulated with polystyrene and gypsum board, and a plywood floor insulated from the ground. The simulation was done for cooling of the floor with various heat transfer coefficients. The structure contains no massive parts and is obviously not suited for structural storage. The simulation results indicate that the cooling only succeeds in increasing the diurnal swing of the interior temperature, with little effect on the peak temperature. These results conform with intuitive expectations.

3.6 Conclusions, Chapter 3

The following conclusions can be stated on the basis of the implementation of – and various simulations with – structural storage.

- The extension of the thermal model to incorporate structural storage appears successful and the results agree with intuitive expectations. In particular these results confirm the contention of Van Aarle and Herman [1] that structural storage is only applicable to massive buildings with well designed shells.

- Incorporation of structural storage in the thermal prediction computer program causes no discernible decrease in the speed of calculation. The extra input data requirements are not excessive but specification of the heat transfer coefficients is somewhat problematic since no general law is available.

- Regarding the verification of the new calculations and procedures; correct results are obtained in limiting cases, but

experimental verification is difficult since the exact value of the convective heat transfer coefficients is not known.

Further verification experiments are required. These experiments must be so designed that the heat transfer coefficient can be directly measured.

It further seems feasible at this stage to instigate a further study, employing the simple model for structural storage presented here, with the objective to investigate the relative merit of structural storage versus other systems e.g. night ventilation. Such a study should consider both capital and running costs, the influence on the design of the building and the relative interior comfort.

REFERENCES Chapter 3

[1] **T. Van Aarle, A. F. E. Herman**, Potential for the air-conditioning of office buildings without mechanical refrigeration, *The South African Mechanical Engineer*, Vol 36 June 1986, pp. 192 – 197.

[2] **C. C. Doyle, A. Johannsen**, Computer–modelling of a structural storage air–conditioning system, *CSIR Division of Production Technology Report*, C/DTP 75.

[3] **J. P. Holman**, Heat Transfer, *Mcgraw–Hill*, 1986 6th Edition ISBN 0–07–Y66459–5.

[4] **ASHRAE**, Handbook Fundamentals, *American Society of Heating Refrigeration and Air–Conditioning Engineers*, 1985.

[5] **J. H. Grobler**, Final Year Thesis, *Department of Mechanical Engineering, University of Pretoria*, Pretoria, 1990.

[6] **R. Zmeureanu, P. Fazio**, Thermal Performance of a Hollow Core Concrete Floor System for Passive Cooling, *Building and Environment*, Vol 23, No 3, pp. 243 – 252, 1988.

SYMBOLS Chapter 3

A Heat transfer area [m^2].
C Empirical coefficient.
c_p Specific heat capacity at constant pressure [kJ/kg·K].
h Air convection coefficient [kW/m^2·K].
h_{sc} Structural cooling convection coefficient [kW/m^2·K].
h_w Convection coefficient [kW/m^2·K].
k Conductivity of fluid [kW/m·K].
L Length of heat transfer surface in direction of flow [m].
m Empirical exponent.
Nu Nusselt number of fluid–surface interface.
n Empirical exponent.
Pr Prandtl number of fluid.
q_w Surface heat flux [kW/m^2].
Re Reynolds number of flow.
R_{sc} Film resistance for structural cooling heat transfer [kW/K].
T_c Bulk structure temperature [^{o}C].
T_{sc} Temperature of air cooling the structure [^{o}C].
T_w Surface temperature [^{o}C].
T_∞ Free–stream fluid temperature [^{o}C].
u_∞ Free–stream velocity of fluid [m/s].
V Windspeed [m/s].

ρ Specific density [kg/m^3].
μ Dynamic viscosity of fluid [kg/s·m].

CHAPTER 4

4 INTER–ZONE HEAT FLOW

One of the more important limitations of the method of Mathews and Richards is the single zone treatment of building thermo–flow. In essence this assumption ignores the possibility of heat flow between adjacent rooms, but instead, assumes all the internal volumes have identical temperatures. While verification experiments indicate that adequate predictions are possible with this assumption [1], the limitations of the single zone assumption can only be accurately determined if a more refined model is available for comparison. It is also the objective of this thesis to refine the program if feasible. For these reasons, a study was instigated to determine theoretically the most convenient method for implementing a multi–zone thermal analysis method. This chapter presents the results of this study.

4.1 Background and Objective of this Chapter

A convenient method for extending the single–zone thermo–flow model to a multi–zone model is provided by the method of the admittance matrix as described by Athienitis [2]. This method, with modifications as suggested here, uses a Thevenin equivalent temperature source which is derived from the single zone model to represent each individual zone (see figure 4.1). These sources are coupled with an admittance matrix which describes the heat flow between the zones. The method requires that each zone be analyzed as a single isolated zone, prior to determining the heat flow between the zones and the final temperatures in each zone. To obtain the inter–zone heat flows and final temperatures the inversion of a matrix of complex numbers is required. The size of this matrix is determined by the number of zones being analyzed.

In this chapter the analysis of the multi–zone system is performed under the assumption of a steady, time invariant thermal network.

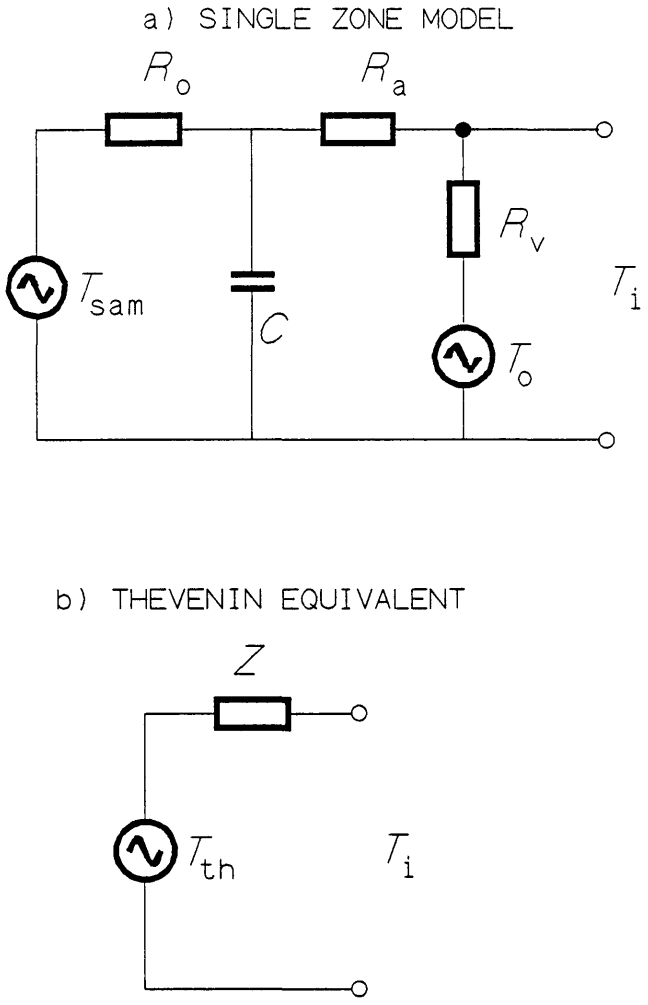

FIGURE 4.1 The Thevenin equivalent temperature of each zone is the interior air temperature which would result when no heat is lost to adjacent zones. The internal impedance is the interior temperature drop per unit of heat lost to adjacent zones.

Nevertheless, the equations and also the considerable complications which arise when the network becomes time dependent, are indicated. In particular, it is shown that while the problem can easily be solved with

transform techniques and matrix algebra in the time invariant case, the more general time variant case requires the solution of a system of differential equations with time dependent coefficients.

It is the objective of this chapter to extend the single zone model and to establish a multi–zone thermal model and analysis technique. The present single zone model serves as the point of departure:– it is assumed valid for every zone in the multi–zone structure. This study then investigates how these individual zones are to be tied together in the multi–zone model. It also investigates methods for rapidly obtaining true or approximate solutions for the resulting complicated network. The solutions are verified by comparison with results obtained from measurements in a model.

4.2 Multi–zone Extension

In the multi–zone building we have a number of inter–reacting zones each of which we assume is basically described by the network of figure 2.1. The interaction between the zones are calculated by coupling the zones with a multi–port network which models the heat exchange between the zones as shown in figures 4.2 to 4.4b. This approach is essentially the same as that described by Athienitis [2]. The multi–port network is easily derived from the physical structures which partition the zones. The solution for the multi–zone network is obtained from the matrix representation of the multi–port network coupled to the Thevenin source of the zone at each port. The Thevenin source representation of a zone is defined as the interior temperature of the zone under adiabatic conditions, i.e. with no heat flow to adjacent zones. With the Thevenin source is associated an internal impedance for each zone which gives the drop in interior temperature of the zone, for each unit of heat which is lost to adjacent zones, as in figure 4.1. The contributions from the partitioning structures are not to be included again in the calculation of

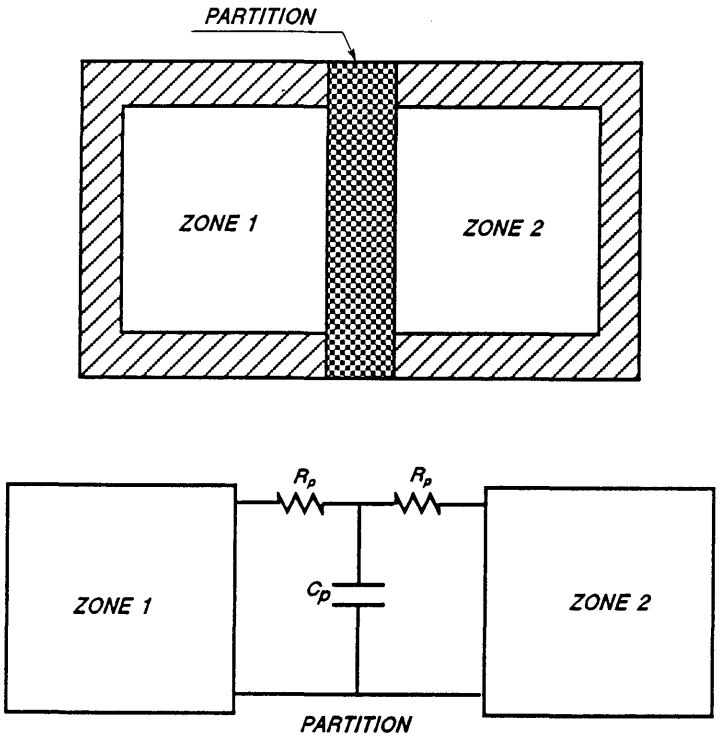

FIGURE 4.2 The lumped representation of the partition between zones is the RCR T section described in chapter 2. The surface coefficients must be included with the branch resistances.

the capacitance or resistance of any zone but internal capacitance in each zone is included in that zones' model as before[1]. In essence, we simply assume the single zone model for each zone and couple the zones with the RCR T section of figure 4.2b, which, according to the

[1]Another alternative is to imagine the partition as split in two and to include the half sections in each zone. The adiabatic line will then run through the middle of the partition. The coupling network between the partitions is then a straight connection without resistances or capacitances. This procedure will be very convenient if the refined model of chapter 2 is used, where internal mass is treated separately. Half the mass of the partition is then included as part of the internal mass of each zone. For the thermal model of Mathews and Richards the procedure in the text is appropriate.

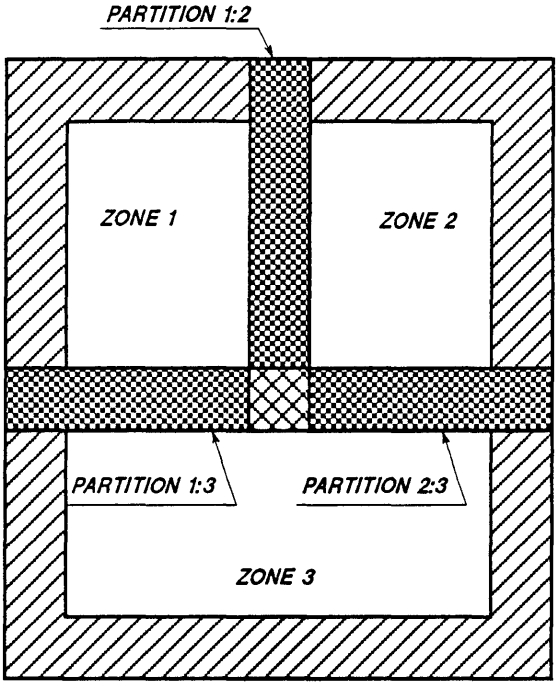

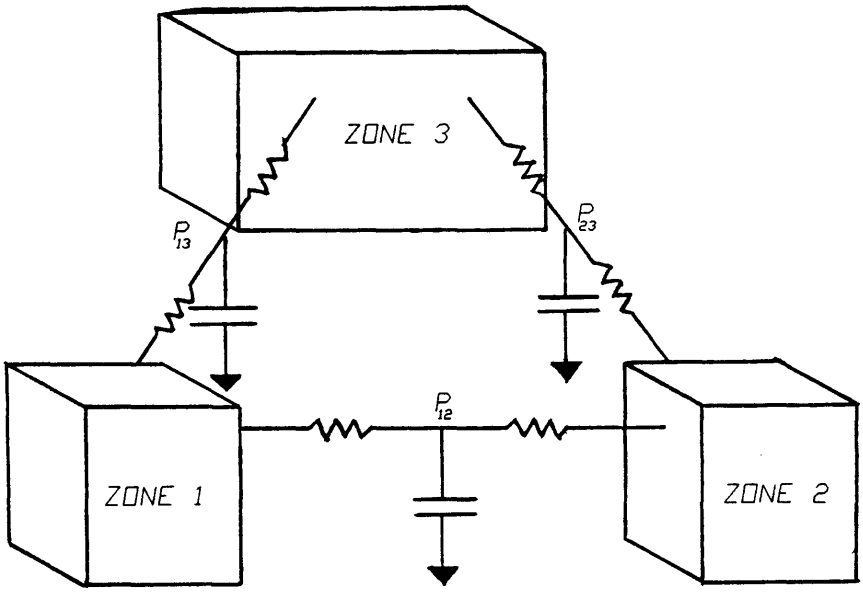

FIGURE 4.3 Representation of a three zone thermal system.

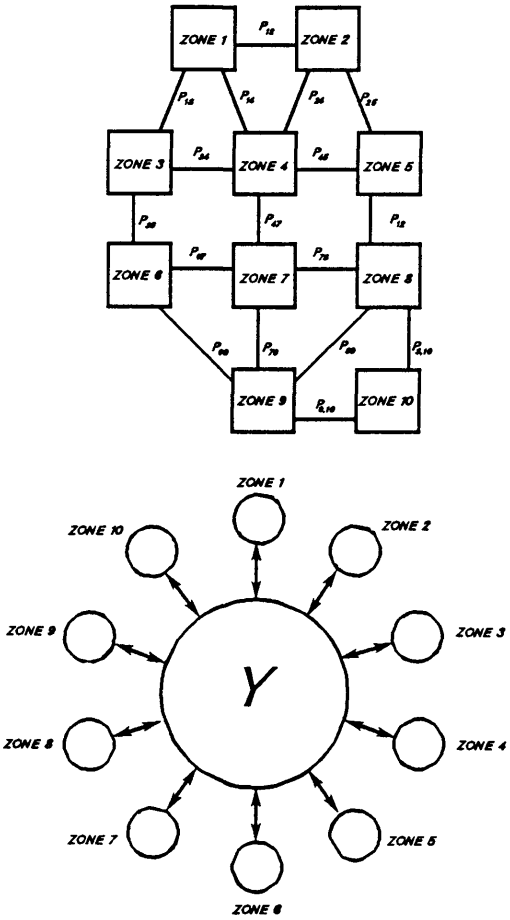

FIGURE 4.4 Representation of a general n–zone thermal system.

discussions on lumping in chapter 2, adequately models the partitions between the zones. To demonstrate: the three zone structure of figure 4.3a is modelled as in figure 4.3b. The general n–zone structure of figure 4.4a is modelled with the network of figure 4.4b where the effect of all the partitions coupling the various zones have been combined in the single admittance matrix Y, and the arrows indicate the internal impedances of the zones.

4.3 Solution of the Multi–Zone Network

The solutions of networks such as in figures 4.2, 4.3 and 4.4 can be obtained by various standard techniques. Particularly well known are mesh (loop) analysis and nodal (cut–set) techniques [3]. These powerful techniques are systematic and guarantee a solution, consequently they are amenable to computer implementation for automatic solution. Many programs exist which can find the solution for an almost arbitrary complex network. The objective here is different, we wish to find a solution for the particular network of interest which can be very quickly evaluated, and which requires no knowledgeable input from the operator as far as the solution of the thermal network is concerned (e.g. identification of network nodes for nodal analysis). In the network of figure 4.4 the operator will be required to identify the zones and the partitions between the zones only. Note that the forcing functions will in general be different for each zone (e.g. west facing zones receive sun energy in the afternoons and east facing zones in the morning).

To increase the speed of computation we use the known solutions, equations 5.23 to 5.34, for the single zone network. The forcing functions of each zone are combined in a Thevenin equivalent source T_e and the effect of the circuit is taken into account by the network operator $\mathfrak{Z}$ as in figure 4.5. The operator representing the partition between the two zones is indicated by $\mathfrak{P}$. The multi–zone thermal circuit is now completely and generally represented by the operators $\mathfrak{Z}$ and $\mathfrak{P}$. This is the 'Y–diakoptic' method as described by Athienitis [2]

with the difference that we prefer to use the Thevenin representation of the sources to the Norton equivalents, because it facilitates appreciation of the effect of the adjacent zones on the indoor temperatures.

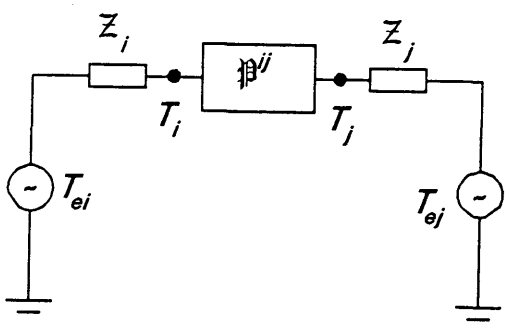

FIGURE 4.5 The Thevenin representation of two coupled zones. The subscript i refers to zone number i, and j to zone number j. The superscript ij refers to the partition between these two zones.

For ease of computation, the operators $\mathfrak{Z}_i$, of all the zones, are combined in a diagonal matrix Z and the partitions operators $\mathfrak{P}^{ij}$ in an admittance matrix Y. The nature of these operators depends on the nature of the circuit parameters and the thermal model. In the most general case, Z and Y are matrices of partial differential operators, coupling the temperatures and heat flows. If the thermal elements are lumped together a lumped circuit description is obtained, and the partial differential equations reduce to ordinary differential equations, with time the only independent variable. If the parameters are linear and time invariant, the Laplace Transform can be applied to the problem and the operators reduce to matrices of rational polynomials in the Laplace

domain variable s, with real coefficients, determined by the constant circuit elements.

The operators can be determined with standard 2–port theory by calculating open circuited voltages and short circuited currents, or, from inspection of the heat flow path. Details are given by Athienitis [2]. We next discuss the nature of these operators in more detail for the linear time invariant case and also for the linear time variant case.

4.3.1 The Zone Circuit Operators and Thevenin Sources

Case 1: time invariant elements, interior temperature calculation

The zone circuit operators and Thevenin sources are determined by reducing the network of heat flows from exterior sources and interior storage to a single effective forcing function T_e operating through an internal impedance $\mathfrak{Z}$. Both the forcing function and impedance will be highly frequency dependent but linear (for linear circuit elements), so that superposition can be used to obtain the total effect of the various forcing functions for all the frequency components they possess. If we assume the thermal model of figure 4.1, the Thevenin sources are just the indoor temperatures calculated from the model, with the assumption that no heat exchange takes place between the different zones. (The open circuit temperature or temperature with adiabatic partition.) In the Laplace domain the Thevenin source for zone number i is from equation 5.1:[2]

$$T_{ei}(s) = \frac{1}{s\tau_{pi} + 1}\left[(s\tau_{zi} + 1)\cdot(R_{ai} + R_{oi})\cdot(T_{oi} + R_{vi}\cdot Q_{ci}) + R_{vi}\cdot(T_{sai} + R_{oi}\cdot Q_{ri})\right]\frac{1}{R_{ai} + R_{vi} + R_{oi}} \qquad (4.1)$$

[2]For full definitions of the symbols see chapter 5. The extra subscript i in (4.1) indicates that the parameters all refer to zone i, the zone currently under consideration.

where:
$$\tau_{pi} = \frac{R_{oi}(R_{ai} + R_{vi})}{R_{oi} + R_{ai} + R_{vi}} \cdot C_i \qquad (4.2)$$

$$\tau_{zi} = \frac{R_{oi} \cdot R_{ai}}{R_{oi} + R_{ai}} \cdot C_i \qquad (4.3)$$

The impedances through which the Thevenin sources operate are the driving point functions at the indoor temperature node, obtained by suppressing all the external sources and calculating the impedance seen from this node into the zone, with all other inter–zone connections removed. From figure 4.6 this impedance is found in the Laplace domain as:

$$\mathfrak{Z}_i = \frac{[R_{oi} + R_{ai} \cdot (R_{oi} sC_i + 1)] \cdot R_{vi}}{R_{oi} + (R_{vi} + R_{ai}) \cdot (R_{oi} sC_i + 1)} \qquad (4.4)$$

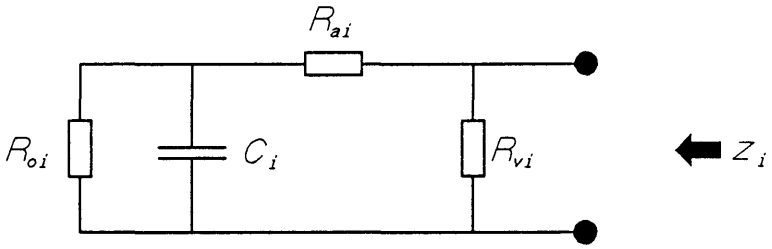

FIGURE 4.6 Method for finding the internal impedance of a zone.

Case 2: time variant elements, interior temperature calculation

When the parameters are variable, considerable complications arise because the circuit differential themselves equations must be used and

the equation for the Thevenin source becomes:

$$T_{ei} + \left[\frac{R_{oi} \cdot R_{vi}}{R_{oi} + R_{ai} + R_{vi}}\right] \cdot \frac{d}{dt}\left[\frac{C_i \cdot (R_{ai} + R_{vi})}{R_{vi}} \cdot T_{ei}\right]$$

$$= \left\{R_{vi} \cdot \left[T_{sai} + R_{oi} \cdot Q_{ri}\right] + (R_{oi} + R_{ai}) \cdot \left[T_{oi} + R_{vi} \cdot Q_{ci}\right] +\right.$$

$$\left. R_{oi} \cdot R_{vi} \cdot \frac{d}{dt}\left[\frac{C_i \cdot R_{ai}}{R_{vi}} \cdot \left[T_{oi} + R_{vi} \cdot Q_{ci}\right]\right]\right\} / \left[R_{ai} + R_{vi} + R_{oi}\right] \quad (4.5)$$

The operator $\mathfrak{Z}_i$ is now defined as that operator, which, when applied to a test load at the terminals of the circuit, will yield the temperature which will arise at the terminals due to the influence of the circuit on the test load (see appendix 4A).

$$T_{test} = \mathfrak{Z}_i\{I_{test}\}$$

$$\mathfrak{Z}_i\{\square\} = \mathfrak{Y}_f^{-1}\left\{\mathfrak{R}_i\{\square\}\right\} \quad (4.6)$$

where:
$$\mathfrak{Y}_f\{\square\} = \mathfrak{D}_t\{\square\} + \mathfrak{R}_i\{\square\} \quad (4.7)$$

$$\mathfrak{D}_t\{\square\} = \frac{1}{R_{vi}} \cdot \square + \frac{d}{dt}\left\{C_i \cdot R_{ai} \cdot \square\right\} \quad (4.8)$$

$$\mathfrak{R}_i\{\square\} = \frac{R_{oi} + R_{ai}}{R_{oi}} \cdot \square + \frac{d}{dt}\left\{C_i \cdot R_{ai} \cdot \square\right\} \quad (4.9)$$

Case 3: time invariant elements, load calculation

For the sensible heat load we find from equation 5.10 when the Laplace

transform is applicable:

$$Q_{ci}(s) =$$

$$\frac{T_{rei}(s\tau_{pi} + 1)\cdot(R_{ai} + R_{vi} + R_{oi}) - R_{vi}\cdot(T_{sai} + R_{oi}\cdot Q_{ri})}{R_{vi}(s\tau_{zi} + 1)\cdot(R_{ai} + R_{vi})} - \frac{T_{oi}}{R_{vi}} \tag{4.10}$$

Where Q_{ci} gives the required convective load to maintain the zone air at temperature T_{rei}.

Case 4: time variant elements, load calculation

For the more general case where the parameters are time dependent the equation is:

$$\left[\frac{R_{oi} + R_{ai}}{R_{oi}\cdot R_{vi}}\right]\cdot(T_{oi} + R_{vi}\cdot Q_{ci}) + \frac{d}{dt}\left\{\frac{R_{ai}\cdot C_i}{R_{vi}}\cdot(T_{oi} + R_{vi}\cdot Q_{ci})\right\}$$

$$= \left[\frac{R_{ai} + R_{vi} + R_{oi}}{R_{vi}\cdot R_{oi}}\right]\cdot T_{ri} + \frac{d}{dt}\left\{\frac{(R_{vi} + R_{ai})\cdot C_i}{R_{vi}}\cdot T_{ri}\right\}$$

$$- \frac{T_{sai} + R_{oi}\cdot Q_{ri}}{R_{oi}} \tag{4.11}$$

In principle the time–variant system can be solved in the same way as the invariant system, but obviously these equations are considerably more complicated than the equations for an invariant system, and solution is extremely difficult. In this study we limit ourselves to demonstrating the solution of the problem in the Laplace domain for time invariant elements.

4.3.2 The Partition Circuit Operators

The interactions between the zones are modelled by assuming the lumped parameter RCR T section of figure 4.2 for the partitions

separating the zones. The lumped parameters are obtained from the distributed characteristics of the structure as explained in chapter 2. More generally, the partition circuit is described by a two port admittance matrix for two zones and a general n–port admittance matrix for n–zones where the admittance matrix includes distributed elements.

In figure 4.2, the heat reservoir of the partition is modelled by C_p. The parameter R_p models the surface plus internal heat flow resistance. The admittance matrix for this 2–port with time invariant parameters is obtained from (2.68):

$$\mathfrak{P}^{ij} = \begin{bmatrix} \mathfrak{P}_{11} & \mathfrak{P}_{12} \\ \mathfrak{P}_{21} & \mathfrak{P}_{22} \end{bmatrix}$$

$$= \frac{1}{R_p \cdot (2+i\cdot\omega\cdot R_p C_p)} \cdot \begin{bmatrix} 1+i\cdot\omega\cdot R_p\cdot C_p & -1 \\ -1 & 1+i\cdot\omega\cdot R_p\cdot C_p \end{bmatrix} \qquad (4.12)$$

When the circuit parameters of the T section are time variant the partition operator must be determined by the application of test sources to the ports, in a manner similar to the method used in appendix 4A to determine the zone impedance operator. The elements of $\mathfrak{P}^{ij}$ will then be differential operators, which, when applied to the temperatures at the ports will yield the differential equations of the heat flow.

When the partition is a compound structure the total effect from all the elements of the partition must be included in the numerical values assigned to the parameters of the T section. For instance, if the partition consists of two distinct surfaces of different construction, the contribution from each surface is easily included by adding the corresponding elements of the two admittance matrices for the two distinct areas (see §2.5.3). For laminated partitions, the equivalent T section for the laminae must first be obtained via (2.62) and (2.63). If heat is also exchanged between the rooms via convection, this

contribution must also be included. In chapter 2 many of these issues are discussed in more detail. Some of the results obtained there are repeated below for convenience.

If the partition is a laminate of n layers of material the contributions of each layer to R_p and C_p are calculated from the following formulae:

$$R_{pc} = \sum_{i=1}^{n} R_{pi} + \frac{1}{h} = \left[\frac{1}{2} \cdot \sum_{i=1}^{n} \frac{\ell_i}{k_i} + \frac{1}{h} \right] \tag{4.13}$$

$$C_{pc} = \left[R_{p1} \cdot C_{p1} + \sum_{j=2}^{n} [R_{pj} + 2 \cdot \sum_{i=1}^{j-1} R_{pi}] \cdot C_{pi} \right] / R_{pc} \tag{4.14}$$

with: $$C_{pi} = c_{pi} \cdot \rho_i \cdot \ell_i$$

The symbols in (3.13) and (3.14) are:

ℓ_i the thickness of layer i
k_i the thermal conductivity of layer i
c_{pi} the specific heat capacity of layer i
ρ_i the specific density of layer i
h film coefficient
and A the area of the partition.

If the partition consists of m different areas (e.g. a wall with a door) the contributions of each area are found from:

$$1/R_{pt} = A_t \cdot \sum_{k=1}^{m} A_k / R_{pk} \tag{4.15}$$

$$C_{pt} = \frac{1}{A_t} \cdot \sum_{k=1}^{n} A_k / R_{pk} \tag{4.16}$$

where the subscript t refers to the total taken over all areas of the partition and k refers to the area of each component.

The contribution due to heat exchange between zones by ventilation can be incorporated by regarding the open areas between the zones, through which ventilation takes place, as areas with no capacity

$$C_{pv} = 0 \tag{4.17}$$

and resistance given by:

$$R_{pv} = R_v/2 \tag{4.18}$$

where the subscript v refers to the T section modelling the effect of the ventilation. R_v is the ventilation resistance which depends on the volume of flow between the zones (See [4,5]).

4.3.3 Solution

The solution consists of first finding the correct admittance matrix and then inverting a matrix equation to find the interior temperatures and loads.

a) Admittance matrix

The solution for time invariant linear parameters is obtained by combining the partition operators $\mathfrak{P}^{ij}$ between each pair of zones in a general admittance matrix, which by definition gives the vector of heat flows from the vector of temperatures, i.e.

$$\boldsymbol{q} = \boldsymbol{Y} \cdot \boldsymbol{T} \tag{4.19}$$

with:

$$\boldsymbol{q} = [q_1 \; q_2 \; q_3 \; \ldots \; q_n]^t$$

the vector of heat flows into each partition and:

$$\boldsymbol{T} = [T_1 \; T_2 \; T_3 \; \ldots \; T_n]^t$$

the vector of temperatures at the surface of each partition. In the above definitions $[\square]^t$ indicates the vector transpose operator.

For two zones, the admittance matrix will correspond with the partition operator

$$Y = \mathfrak{P}^{ij} \tag{4.20}$$

but for three or more zones the elements of Y is combined from the elements of the $\mathfrak{P}^{ij}$ for each pair of interconnected zones. The elements of Y can normally be found by inspection of the interconnections between the zones, since at each zone's port, the flows through all the partitions connecting this zone to other zones, add together. As an illustration of the method, the admittance matrix for the three zone structure of figure 4.3 is:

$$Y = \begin{bmatrix} (\mathfrak{P}_{1\,1}{}^{12}+\mathfrak{P}_{11}{}^{13}) & \mathfrak{P}_{1\,2}{}^{1\,2} & \mathfrak{P}_{1\,2}{}^{1\,3} \\ \mathfrak{P}_{21}{}^{1\,2} & (\mathfrak{P}_{22}{}^{1\,2}+\mathfrak{P}_{11}{}^{23}) & \mathfrak{P}_{1\,2}{}^{2\,3} \\ \mathfrak{P}_{21}{}^{1\,3} & \mathfrak{P}_{2\,1}{}^{2\,3} & (\mathfrak{P}_{22}{}^{1\,3}+\mathfrak{P}_{22}{}^{23}) \end{bmatrix} \tag{4.21}$$

In (3.21) the superscripts refer to the zones and the subscripts to the matrix element, i.e. $\mathfrak{P}_{11}{}^{12}$ refers to the element in row 1, column 1 of the partition between zones 1 and 2. To demonstrate:– the first element is obtained from figure 4.3 by noting that zone 1 is coupled to both zones 2 and 3. The total flow from this zone is therefore the sum of the flows to the two zones, and consequently, the first element is given by the sum of the first elements of the partitions from zone 1 to zone 2 and from zone 1 to zone 3.

b) Interior Temperature

With the Thevenin sources for each zone and the admittance matrix giving the coupling between the zones known, the final solution for the interior temperature in each zone is obtained by matrix inversion. Define

$$T_e = [T_{e1}\ T_{e2}\ T_{e3}\ \ldots\ T_{en}]^t \tag{4.22}$$

a vector of Thevenin interior temperatures for the zones,

and $$Z = \begin{bmatrix} \mathfrak{Z}_i & 0 \\ 0 & \mathfrak{Z}_j \end{bmatrix} \tag{4.23}$$

a diagonal matrix with the internal impedances of the zones. From the definition of the admittance matrix Y (4.19) we have:

$$q = Y \cdot T \tag{4.24}$$

But from the circuit in figure 4.5:

$$T = T_e - Z \cdot q = T_e - Z \cdot (Y \cdot T) \tag{4.25}$$

Finally solving for T from this equation gives the interior temperature of the couples zones:

$$T = [I + Z \cdot Y]^{-1} \cdot T_e \tag{4.26}$$

Equation (4.26) gives the final answer for the interior temperature T, in terms of the interior temperature T_e when the zones were isolated from each other. In this equation, the contribution from the partitions is represented by Y and the influence of the shells of the zones (internal impedance) is given by Z.

c) Sensible Heat Load

To calculate the sensible load to maintain a given temperature T_{re} in the zones, the required Thevenin sources for the zones T_e is solved from (4.26) with $T = T_{re}$ the specified indoor temperatures. From the required Thevenin sources, the required convective load is obtained exactly as in the case of the single zone model, except that the required interior temperature is taken as the required Thevenin temperature, and the partitions are ignored. Thus setting $T = T_{ir}$ in (4.26) and solving

for $T_e = T_{er}$, the required Thevenin temperature, gives:

$$T_{er} = [I + Z*Y] * T_{ir} \tag{4.27}$$

With T_{er} known the heat load is calculated for each zone from (4.10).

4.4 Computer Implementation

The obvious method to calculate the final indoor temperature for the multi–zone network is via (4.26) with the matrix inversion calculated via the Gauss–Jordan algorithm or a similar procedure. This will involve finding the inverse of a $n \times n$ complex matrix where n is the number of zones present. The method is illustrated in appendix 4B. Note that when the mean temperatures on each side of the partition are equal no mean flow of heat across the partition takes place. Nevertheless, the partition still influences the swing as the capacitance of the partition contributes to the dampening of the swing. The multi–zone matrix calculation must still be carried out to obtain the correct indoor temperature.

The sensible load calculation via equation (4.27) is quite straight forward.

4.4.1 Time Invariant System

For a time invariant system the multi–zone implementation is rather straightforward and is designed to be a natural natural extension to the program of Mathews and Richards, in the following manner:

To find INTERIOR TEMPERATURE in the zones

- Specify each zone exactly as with the single zone model, but do not include contributions from the partitions, i.e. treat each zone as though the partition is a perfect insulator.

- Calculate the interior temperature in each zone with the partitions regarded as insulators.[3] Combine the temperatures in a vector; definition (4.22).
- Find the impedance matrix Z for the various zones; definition (4.23).
- Find the admittance matrix $\mathfrak{P}^{ij}$ for each partition and combine them in the admittance matrix Y; (4.21).
- Find the indoor temperatures via matrix inversion; (4.26).

To find SENSIBLE LOADS (assuming interior temperatures have been found first).

- Specify the required indoor temperature for each zone.
- Solve for the values of the Thevenin sources; (4.27).
- Find the convective load that will give the specified indoor temperature in each zone, with the partition regarded as an insulator; (4.10)

4.4.2 Time Variant System

Implementation of the general case with variable parameters are similar except that the differential equations with variable coefficients must be solved instead of polynomials in s. Because $\mathfrak{Z}_i$ is determined by (4.6) to (4.9), equations (4.26) and (4.27) must be solved with Z and Y re–interpreted as impedance operators, yielding differential equations coupling T to T_e and T_{er} to T_r. Instead of obtaining the solution by matrix inversion and multiplication, these differential equations will have to be solved, possibly by numerical means.

An alternative approximate procedure is to use a time dependent definition of $Z = Z(t)$ and then to carry out the matrix inversion at

[3] Up to here the procedure is exactly as with the single zone model.

each time instant. The procedure is:

- Calculate the insulated interior temperatures (Thevenin temperatures) with the present variable parameter network solutions.
- Assume that the parameters of the partition are invariant i.e. doors are not opened and closed between the zones etc.[4]
- Define $\mathfrak{Z}_i(t)$ as the complex time dependent ratio between test voltage and test current as opposed to equation 3.6. Define $Z = Z(t)$; Definition (4.23).
- Carry out the matrix inversion for every time instant to find the interior temperature; (4.26).
- Find the load by matrix multiplication for every time instant, as before.

This procedure will be approximate only as the derivatives of the time dependent circuit elements also contribute terms to the differential equations. These terms are ignored in the above procedure. In the actual solution of the time variant equations (4.5 and 4.11) it is expedient to solve the equivalent equations for the energy stored in the massive structure, rather than the equations for temperatures and heat flows. The stored heat is a reasonably smooth function of time with small derivatives, (see chapter 5). For this reason this approximate technique can provide reasonable answers. But a considerable amount of computation is still required since an nxn matrix inversion is required at each time instant. Another, more accurate alternative, would be to write the differential equations as difference equations and to use standard numerical techniques for solution. The investigation of these techniques are, however, outside the scope of this study.

[4]This assumpion is not essential but it will reduce the complexity of the solution. When the parameters of the partition are also functions of time, the admittance matrix Y also becomes a function of time $Y(t)$.

4.5 Verification

Obviously the best method for establishing the validity of the model is to obtain measurements in actual buildings. Such an experiment will require detailed logging of temperatures, loads and all human activity in the various zones and, consequently, will be very difficult and expensive to execute. A second best, more practical method is to use a model of a building. Such an experiment is described here.

4.5.1 Experimental results

To verify the procedure for combining the zones an experiment was conducted in a model consisting of two similar zones which could be interconnected or isolated with various partitions. The model was placed in a laboratory beneath ground level where the indoor temperature was found to be almost constant. To test the multi–zone solution method, the zones were first insulated from each other and a heat source was placed in one zone. To ensure a uniform interior temperature a small fan was placed in each zone stirring the air continuously. The power dissipation of the fan was considered negligible. The temperature changes due to the heat source being switched on and off were recorded in both zones with a thermograph. The heat storage capacity of the thermographs were taken into account. The results from this measurement is given in figures 4.7a&b. In figure 4.7a we have the temperature in the active zone and in figure 4.7b in the passive zone. Clearly, almost no heat transfer between the two zones took place. The measured temperature swing in zone 1 must therefore correspond to the Thevenin temperature T_{e1} of (4.10) while for zone 2 we have $T_{e2} = 0$. (We disregard the constant mean component.) To determine the interaction between the zones, a semi–conducting partition was next placed between the zones and the temperature in each zone was again recorded. The results from this second experiment is shown in figures 4.8a and 4.8b, and clearly some of the heat is transferred to zone 2, which now also exhibits temperature swings, while the swing in zone 1 is reduced. If the multi–zone analysis technique is capable of correctly

predicting the change in temperature swings between figures 4.7 and 4.8, in each zone, it will be verified for the two zone model. By measuring the Thevenin temperature in this way, we are able to circumvent any calibration inaccuracies in the thermographs and can obtain accurate numerical values for the zone parameters, as explained in the next section.

4.5.2 Application of multi–zone procedure to model

To apply the analysis technique to the model we need an accurate thermal model of the type of figure 4.1. The values of the resistors and capacitances in the model can be found from the physical construction, but since we only wish to verify the multi–zone procedure, and not the thermal modelling, it is easier and more accurate to obtain the zone model directly from the measured response when the zones are isolated. Note in figure 4.7 the temperature swing corresponds to the step–response of a single time constant RC network. By definition the time constant τ is the time until 63% of the final value is attained and from the figure this is estimated to be 2.7 hours. The internal impedance can be found from figure 4.6 by calculating the driving point impedance as seen at the interior air node, with all sources suppressed and no ventilation:

$$\mathfrak{Z}_1 = \mathfrak{Z}_2 = R_a + \frac{R_o}{\tau \cdot s + 1} \qquad (4.28)$$

Besides the value of the time constant, the values of R_a and R_o are required to find the impedance $\mathfrak{Z}$. To obtain the value of R_o, the measured temperature swing is compared with the theoretical temperature swing when the zones are isolated. The step response to a 50 W radiative source of the circuit of figure 4.1, in the absence of ventilation is:

$$T(t) = 50 \cdot R_o \cdot (1 - e^{-t/\tau}). \qquad (4.29)$$

The measured amplitude of the step response is 9°C from which it follows that R_o = 180 K/kW. The value of R_a is determined by the inside film coefficient. This is the only parameter of the zone model which is undetermined by the measurements. In general it is extremely difficult to determine surface heat transfer coefficients. In the model, one side of the partition is subject to intense radiation from the heat source and convective transfer plays a minor role. On the other side, in the passive zone, the heat transfer takes place both through radiation and convection. Determination of the heat transfer coefficients requires detailed knowledge of the air movement in each zone and also of the difference in temperature between the various surfaces. In the verification calculation it was assumed the film coefficient in zone 1 is very large, due to the radiation directly heating the surface. The film coefficient in zone 2 was taken as 12 W/m²·K, a value based on a (probably debatable) calculation in appendix 4C.

The RC elements of the T section representing the semi–conducting partition is obtained from the thermal parameters of the construction material and the area of the partition (under the assumption that the film coefficient in zone 1 is very large):

$$R_p = \frac{1}{2} \cdot \left[\frac{1}{k} + \frac{1}{h_2}\right] \cdot \frac{1}{A} = 116.9 \text{ K/kW}$$

$$C_p = c_p \cdot \rho \cdot \ell \cdot A = 6.6 \text{ kJ/K}$$

where: k = 0.62 W/m·K thermal conductivity
h_2 = 12 W/m²·K partition film coefficient in zone 2[5]
A = 0.419 m² area of the partition
c_p = 0.83 kJ/Kg·K specific heat capacity
ρ = 2100 kg/m³ specific density of asbestos
and ℓ = 9 mm thickness of the partition.

[5]Determined from radiative and convective heat transfer in appendix 4.C.

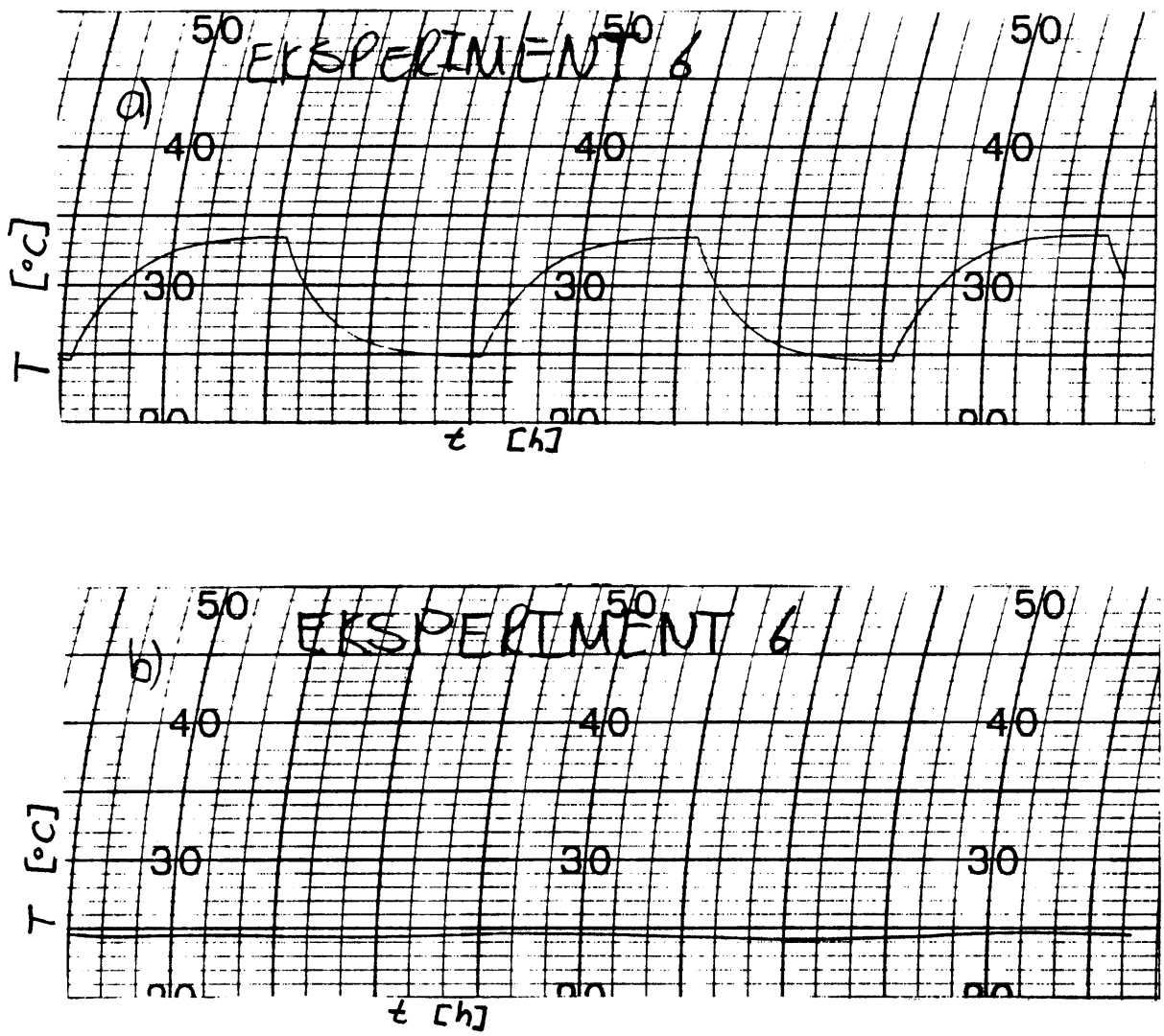

FIGURE 4.7 Measured temperatures in the zones with insulation between the zones, a) is the temperature in the zone with the heat source, b) is the temperature in the passive zone. The horizontal axis is marked every 2 hours.

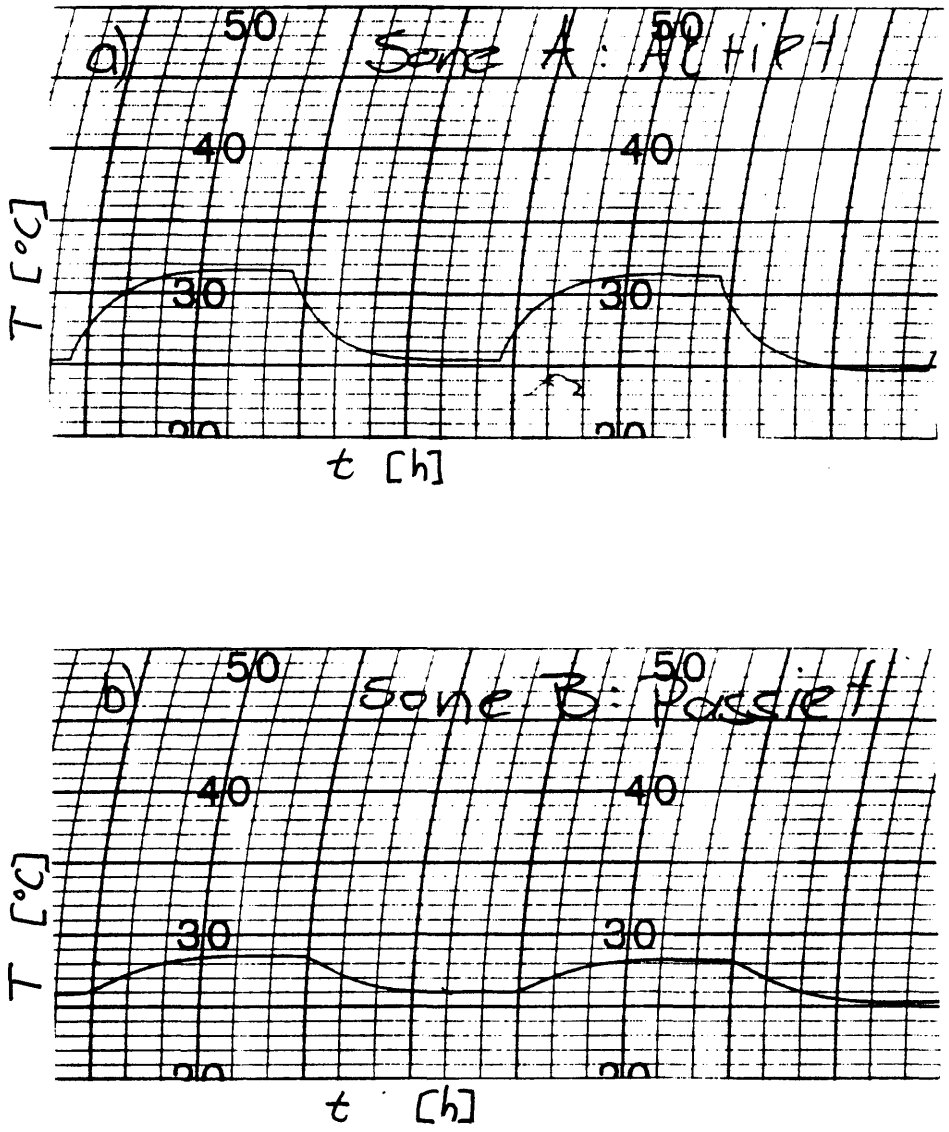

FIGURE 4.8 Measured temperatures in the zones with a partially conducting partition, a) is the temperature in the zone with the heat source, c) is the temperature in the passive zone. The horizontal axis is marked every 2 hours.

With these numerical values of the circuit elements the multi–zone analysis can proceed for each frequency component of the square wave forcing function. The calculation is carried out in appendix 4D and the predicted temperature swings in the zones are 6 °C in zone 1 and 2.5 °C in zone 2. These values are essentially the same as the measured swings given in figures 4.8a & b so that the predictions compare very favorably with the actual temperatures.

To investigate the sensitivity of the procedure with respect to the unknown surface coefficients, the calculation was repeated for a heat transfer coefficient $h_2 = 20$ W/m²·K. The predicted temperature in zone 1 was 6 °C and in zone 2, 3 °C. Bearing in mind the difficulty of determining the correct heat transfer coefficient the procedure appears to be well verified by the measurements in the model.

5.6 Conclusions, Chapter 4

This part of the study has been successful in as much as it proved possible to find a reasonably effective and accurate method to obtain the solution to the multi–zone thermal model when the parameters of the circuit are time invariant. The method is also applicable to the more general time variant case but in this case considerable imple–mentational difficulties arise which will result in cumbersome and time consuming computations. It has not been determined whether a more practical approach to the time dependent problem exists.

Before the techniques suggested in this program can be implemented a careful analysis of the data input, output and required operator interface must be made in order to design a logical and user friendly multi–zone program. Note however that the method facilitates separate calculation of each zone's influence followed by combining the zones via the partition admittance matrix and calculation of the final temperatures. This procedure is exactly the same as the current method of combining the energy requirements of the various zones in the program.

Nevertheless, an extensive rethink of especially the output procedures is required since currently the temperature results for each zone are found before the zones are combined whereas the multi–zone procedure will only supply the final temperature results after the zones have been combined. Furthermore, before the zones can be combined the partitions and heat flow paths between the zones must be identified and described.

Final verification of the method and it's implementation will be required. This will entail extensive measurements in various types of existing buildings and models. Note however, that the procedure for combining the zones is a mathematically exact procedure; if any discrepancies surface, they must be attributed to the models describing the zones or the partitions, or to inadequacies in the numerical implementation.

The detailed implementation and effectiveness of the method for time varying circuit parameters have not been investigated in this study. It is also possible that in this instance a more effective calculation procedure than that suggested here exists. These questions will take considerable effort and time to investigate properly, since few convenient mathematical techniques for treating systems of differential equations with variable coefficients exist. A numerical and\or iterative approach might possibly be more rewarding.

REFERENCES Chapter 4

[1] **E. H. Mathews, P. G. Richards**, A Tool for Predicting Hourly Air Temperature and Sensible Energy Loads in Buildings at Sketch Design Stage, *Energy and Buildings*, Vol 14 No 1 pp 61–80.

[2] **A. K. Athienitis**, Application of Network Methods to Thermal Analysis of Passive Solar Buildings in the Frequency Domain, *PhD Thesis, University of Waterloo*, Ontario 1985.

[3] **L. O. Chua, P.–M. Lin**, Computer–Aided Analysis of Electronic Circuits, *Prentice–Hall, Inc.*

[4] **D. Hill, A. Kirkpatrick, P. Burns**, Analysis and Measurements of Interzonal Natural Convection Heat Transfer in Buildings, *Journal of Solar Energy Engineering*, Vol 108 No 3 August 1986,pp. 178 – 184.

[5] **S. A. Barakat**, Inter–Zone Convective Heat Transfer in Buildings: A Review, *Journal of Solar Energy Engineering*, Vol 109 No 71 May 1987, pp. 71 – 76.

SYMBOLS Chapter 4

A	Load contribution factor of interior air temperature.
$\mathscr{A}$	Element of transmission matrix.
a	Temperature contribution factor of out door air temperature.
B	Load contribution factor of sol–air temperature.
$\mathscr{B}$	Element of transmission matrix.
b	Temperature contribution factor of convective source.
C	Heat storage capacitance per unit area of shell [kJ/m^2·K], load contribution factor of radiative source.
C_p	Heat storage capacitance of partition.[kJ/m^2·K]
$\mathscr{C}$	Element of transmission matrix.
c	Temperature contribution factor of sol–air temperature.
c_p	Specific heat capacity [kJ/kg·K].
D	Load contribution factor of out door air temperature.
$\mathscr{D}$	Element of transmission matrix.
d	Temperature contribution factor of radiative source.
h_i	Internal wall film coefficient [W/m^2·K].
h_o	External wall film coefficient [W/m^2·K].
i	Imaginary number, index – natural number.
I_t	Test current.
k	Thermal conductivity [W/m·K].
ℓ	Wall thickness [m].
Q_c	Convective load [kW/m^2].
Q_r	Radiative load [kW/m^2].
R_a	Film heat resistance from interior surface of shell to interior air [K·m^2/kW].
R_o	Shell partial heat resistance [K·m^2/kW], sometimes divided by shell area [K/kW].
R_p	Partial heat resistance of partition [K/kW].
R_v	Ventilation equivalent resistance [K·m^2/kW].

R_v	Ventilation equivalent resistance between zones [K/kW].
s	Laplace domain independent variable [1/h].
$\boldsymbol{T}$	Transmission matrix, vector of temperatures.
T	Temperature [°C].
T_c	Mean structure temperature [°C].
T_e	Effective forcing temperature [°C].
T_{ei}	Thevenin equivalent temperature in zone i [°C].
T_i	Interior air temperature [°C].
T_{ir}	Required (thermostat) interior air temperature [°C].
T_o	Outdoor air temperature [°C].
T_{sa}	Effective Sol–Air temperature [°C], combined contribution from all external surfaces.
T_t	Test temperature [°C].
t	Time [h].
q	Heat flux density [kW/m²].
$\boldsymbol{U}$	Vector of temperature and heat flow.
$\boldsymbol{Y}$	Admittance matrix.
x	Spatial dimension [m].
ω	Radian frequency [rad/h].
ρ	Specific density [kg/m³].
τ_z	Time constant of network zero [h].
τ_p	Time constant of network pole [h].
$\mathfrak{D}_t$	A linear operator.
$\mathfrak{P}^{ij}$	Partition between zones i and j (operator).
$\mathfrak{R}_i$	A linear operator.
$\mathfrak{Y}_f$	A linear operator.
$\mathfrak{Z}_i$	Internal impedance of zone i (operator) [K·m²/kW].

APPENDIX 4A

Derivation of the 3 impedance operator.

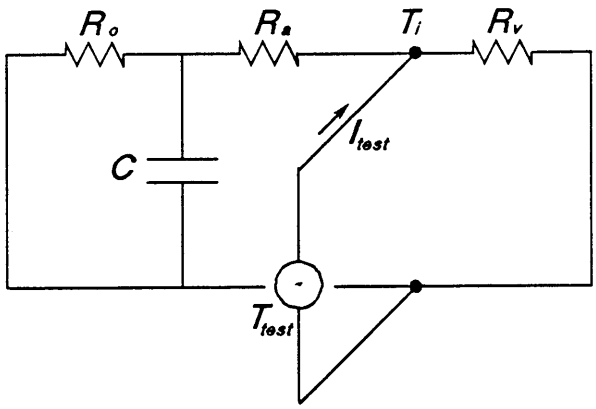

Figure 4A

In figure 4A we apply the test source T_t to the terminals of the interior air node. The current into the circuit from this test source is I_t and is given by:

$$I_t = T_t/R_v + I_a \tag{A.1}$$

$$I_a = I_c + I_o \tag{A.2}$$

$$I_c = \frac{d(C\cdot T_c)}{dt}, \quad I_o = \frac{T_c}{R_o} \tag{A.3}$$

But
$$T_c = T_t - I_a\cdot R_a \tag{A.4}$$

so
$$I_a = \frac{d}{dt}\left\{C\cdot(T_t - I_a\cdot R_a)\right\} + \frac{T_t - I_a\cdot R_a}{R_o}$$

This equation can be written in the form:

$$I_a\cdot\left[1 + \frac{R_a}{R_o}\right] + \frac{d}{dt}\left\{C\cdot R_a\cdot I_a\right\} = \frac{d}{dt}\left\{C\cdot T_t\right\} + \frac{T_t}{R_o} \tag{A.5}$$

If we now define: $$\mathfrak{D}_i\{i\} = \left[\frac{R_o + R_a}{R_o}\cdot i + \frac{d}{dt}\left\{C\cdot R_a\cdot i\right\}\right]$$

$$\mathfrak{D}_t\{i\} = \left[\frac{i}{R_o} + \frac{d}{dt}\left\{C\cdot i\right\}\right]$$

equation (A.5) becomes:

$$\mathfrak{D}_i\{I_a\} = \mathfrak{D}_t\{T_t\} \tag{A.6}$$

and with equation B.1 this is written as:

$$\mathfrak{D}_i\left\{I_t - \frac{T_t}{R_a}\right\} = \mathfrak{D}_t\{T_t\} \tag{A.7}$$

Note however that $\mathfrak{D}_i$ is a linear operator so from this equation can be solved for I_t in the following way:

$$\mathfrak{D}_i\{I_t\} = \mathfrak{D}_t\{T_t\} + \mathfrak{D}_i\left\{\frac{T_t}{R_a}\right\} \tag{A.8}$$

Finally with:

$$\mathfrak{D}_f\{\square\} = \mathfrak{D}_t\{\square\} + \mathfrak{D}_i\left\{\frac{\square}{R_a}\right\} \tag{A.9}$$

we obtain:

$$T_t = \mathfrak{D}_f^{-1}\{\mathfrak{D}_i\{I_t\}\} = \mathfrak{Z}\{I_t\} \tag{A.10}$$

In the above derivation we have used the inverse of an operator as though it always exists and can be found. In practice finding the inverse of a differential operator is not a trivial task and may well be impossible. In general the differential equation obtained by the application of the operator must be solved and the inverse of the resultant solution must be obtained. It is not at all certain that this is possible in practice. The investigation of these questions fall outside the scope of this study and we shall not attempt to obtain the solution for the general time variant case.

APPENDIX 4B

Demonstration of multi-zone solution via matrix inversion.

A) Calculation of temperature and heat flow swings.

Define units: length mass time temperature

$m \equiv 1L \quad kg \equiv 1M \quad s \equiv 1T \quad C \equiv 1Q$

$J \equiv kg \cdot m^{2} \cdot s^{-2} \qquad W \equiv J \cdot s^{-1}$

$kJ \equiv J \cdot 10^{3} \qquad kW \equiv W \cdot 10^{3}$

$h \equiv 60 \cdot 60 \cdot s \qquad rad \equiv 1$

$deg \equiv \frac{\pi}{180} \cdot rad$

Resistance units: $\Omega \equiv m^{2} \cdot C \cdot kW^{-1}$

Capacitance units: $F \equiv kJ \cdot m^{-2} \cdot C^{-1}$

Define frequency 1/24h:

$f \equiv 1 \cdot 24^{-1} \cdot h^{-1}$

$\omega \equiv 2 \cdot \pi \cdot f \qquad s \equiv i \cdot \omega$

Two zone demonstration. The upper value of the vectors below applies to zone 1 and the bottom value to zone 2. The zones are physically equivalent except that zone 2 has 10 times the shell capacitance of zone 1.

Outside temperature swings: $To := \begin{bmatrix} 15 \\ 15 \end{bmatrix} \cdot C$

$Tsa := \begin{bmatrix} 25 \\ 25 \end{bmatrix} \cdot C$

Shell resistances: $Ro := \begin{bmatrix} 100 \\ 100 \end{bmatrix} \cdot \Omega$

Internal surface coefficients: $Ra := \begin{bmatrix} 10 \\ 10 \end{bmatrix} \cdot \Omega$

Ventilation resistances: $Rv := \begin{bmatrix} 200 \\ 200 \end{bmatrix} \cdot \Omega$

Heat storage capacitance: $Ca := \begin{bmatrix} 200 \\ 2000 \end{bmatrix} \cdot F$

Thermal time constants:

$$\tau p := \left[\frac{Ro\cdot(Ra + Rv)\cdot Ca}{Ro + Ra + Rv}\right]$$

$$\tau p = \begin{bmatrix}3.8\\37.6\end{bmatrix}\cdot h$$

$$\tau z := \left[\frac{Ro\cdot Ra\cdot Ca}{Ro + Ra}\right]$$

$$\tau z = \begin{bmatrix}0.5\\5.1\end{bmatrix}\cdot h$$

Calculated interior Thevenin temperatures:

$$Ti(s) := \left[\frac{Rv\cdot Tsa + (s\cdot\tau z + 1)\cdot(Ra + Ro)\cdot To}{(s\cdot\tau p + 1)\cdot(Ra + Rv + Ro)}\right]$$

$$Ti(s) = \begin{bmatrix}11.237 - 10.368i\\0.926 - 2.083i\end{bmatrix}\cdot C$$

Source internal impedances:

$$Zi(s) := \left[\frac{Rv\cdot(Ro + Ra\cdot(Ro\cdot s\cdot Ca + 1))}{(Rv + Ra)\cdot(Ro\cdot s\cdot Ca + 1) + Ro}\right]$$

$$Zi(s) = \begin{bmatrix}40.702 - 30.719i\\10.15 - 6.173i\end{bmatrix}\cdot\Omega$$

$$Z(s) := \begin{bmatrix}Zi(s) & 0 & 0\cdot\Omega\\ & Zi(s) & \\0\cdot\Omega & & 1\end{bmatrix}$$

Partition admittance matrix:

The partition consists of a T network with arms of resistance Rp and trunk of capacitance Cp.

$$Rp := 50\cdot\Omega$$

$$Cp := 50\cdot F$$

$$Y(s) := \frac{1}{Rp\cdot(Rp\cdot s\cdot Cp + 2)}\cdot\begin{bmatrix}Rp\cdot s\cdot Cp + 1 & -1\\-1 & Rp\cdot s\cdot Cp + 1\end{bmatrix}$$

$$Y(s) = \begin{bmatrix}0.01 + 9.02\cdot10^{-4}\,i & -0.01 + 9.02\cdot10^{-4}\,i\\-0.01 + 9.02\cdot10^{-4}\,i & 0.01 + 9.02\cdot10^{-4}\,i\end{bmatrix}^{-1}\cdot\Omega$$

Multizone solution via matrix inversion:

$$I := \begin{bmatrix} 1 & 0 \\ 0 & 1 \end{bmatrix} \qquad T(s) := (I + Z(s) \cdot Y(s))^{-1} \cdot Ti(s)$$

Interior temperature swing: $Ts := T(s)$

$$Ts = \begin{bmatrix} 8.716 - 6.633i \\ 1.303 - 2.941i \end{bmatrix} \cdot C$$

$$\left| \begin{bmatrix} Ts \\ 0 \end{bmatrix} \right| = 10.953 \cdot C \qquad \arg\left(\begin{bmatrix} Ts \\ 0 \end{bmatrix} \right) = -37.272 \cdot deg$$

$$\left| \begin{bmatrix} Ts \\ 1 \end{bmatrix} \right| = 3.217 \cdot C \qquad \arg\left(\begin{bmatrix} Ts \\ 1 \end{bmatrix} \right) = -66.098 \cdot deg$$

Heatflow between zones: $Q(s) := Y(s) \cdot T(s)$

$$Q(s) = \begin{bmatrix} 0.084 - 0.029i \\ -0.065 + 0.045i \end{bmatrix} \cdot kW \cdot m^{-2}$$

$$\left| \begin{bmatrix} Q(s) \\ 0 \end{bmatrix} \right| = 0.088 \cdot kW \cdot m^{-2} \qquad \arg\left(\begin{bmatrix} Q(s) \\ 0 \end{bmatrix} \right) = -18.935 \cdot deg$$

$$\left| \begin{bmatrix} Q(s) \\ 1 \end{bmatrix} \right| = 0.079 \cdot kW \cdot m^{-2} \qquad \arg\left(\begin{bmatrix} Q(s) \\ 1 \end{bmatrix} \right) = 145.068 \cdot deg$$

B) Solution for required heat load.

Required interior temperatures: $Tr := \begin{bmatrix} 24 \\ 24 \end{bmatrix} \cdot C$

Required Thevenin sources: $Tth(s) := (I + Z(s) \cdot Y(s)) \cdot Tr$

$$Tth(s) = \begin{bmatrix} 25.489 + 1.641i \\ 24.307 + 0.415i \end{bmatrix} \cdot C$$

$$\left| Tth(s)_0 \right| = 25.542 \cdot C \qquad \arg\left[Tth(s)_0 \right] = 3.683 \cdot deg$$

$$\left| Tth(s)_1 \right| = 24.311 \cdot C \qquad \arg\left[Tth(s)_1 \right] = 0.978 \cdot deg$$

Heat flow into partition: $Qr(s) := Y(s) \cdot Tth(s)$

$$Qr(s) = \begin{bmatrix} 0.014 + 0.057i \\ -0.01 + 0.033i \end{bmatrix} \cdot kW \cdot m^{-2}$$

$$\left| Qr(s)_0 \right| = 0.059 \cdot kW \cdot m^{-2} \qquad \arg\left[Qr(s)_0 \right] = 76.225 \cdot deg$$

$$\left| Qr(s)_1 \right| = 0.034 \cdot kW \cdot m^{-2} \qquad \arg\left[Qr(s)_1 \right] = 106.304 \cdot deg$$

C) Calculation of mean temperature and heat flow.

Outside mean temperatures:

$$Tom := \begin{bmatrix}15\\15\end{bmatrix} \cdot C$$

$$Tsam := \begin{bmatrix}25\\25\end{bmatrix} \cdot C$$

Calculated interior Thevenin temperatures:

$$Tim := \overrightarrow{\left[\frac{Rv \cdot Tsam + (Ra + Ro) \cdot Tom}{Ra + Rv + Ro}\right]}$$

$$Tim = \begin{bmatrix}21.452\\21.452\end{bmatrix} \cdot C$$

Source internal impedances:

$$Zim := \overrightarrow{\left[\frac{(Ro + Ra) \cdot Rv}{Rv + Ra + Ro}\right]}$$

$$Zim = \begin{bmatrix}70.968\\70.968\end{bmatrix} \cdot \Omega$$

$$Zm := \begin{bmatrix}Zim & 0 \cdot \Omega\\ 0 \cdot \Omega & Zim\end{bmatrix}$$

Partition admittance matrix:

$$Ym := \frac{1}{Rp \cdot 2} \cdot \begin{bmatrix}1 & -1\\-1 & 1\end{bmatrix}$$

$$Ym = \begin{bmatrix}0.01 & -0.01\\-0.01 & 0.01\end{bmatrix} \cdot \Omega^{-1}$$

Multizone solution via matrix inversion:

$$I := \begin{bmatrix}1 & 0\\0 & 1\end{bmatrix} \qquad Tm := (I + Zm \cdot Ym)^{-1} \cdot Tim$$

Mean Interior temperature:

$$Tm = \begin{bmatrix}21.452\\21.452\end{bmatrix} \cdot C$$

Heatflow between zones: $Qm := Ym \cdot Tm$

$$Qm = \begin{bmatrix}0\\0\end{bmatrix} \cdot kW \cdot m^{-2}$$

D) Solution for required mean heat load.

Required interior temperatures: $Tr := \begin{bmatrix} 24 \\ 24 \end{bmatrix} \cdot C$

Required Thevenin sources: $Tthm := (I + Zm \cdot Ym) \cdot Tr$

$$Tthm = \begin{bmatrix} 24 \\ 24 \end{bmatrix} \cdot C$$

Heatflow into partition: $Qh := Ym \cdot Tthm$

$$Qh = \begin{bmatrix} 0 \\ 0 \end{bmatrix} \cdot kW \cdot m^{-2}$$

APPENDIX 4C

Estimation of the interior heat transfer coefficient for the two zone experiment.

Reference: Holman JP
Heat Transfer
McGraw-Hill 1986
Chapter 5

Define units:

length	mass	time	temperature
$m \equiv 1L$	$kg \equiv 1M$	$s \equiv 1T$	$K \equiv 1Q$

$J \equiv kg \cdot m^2 \cdot s^{-2}$ $\quad W \equiv J \cdot s^{-1}$

$kJ \equiv J \cdot 10^3$ $\quad kW \equiv W \cdot 10^3$

$mm \equiv m \cdot 10^{-3}$

Properties of air at 300 K (from Holman Table A-5):

Kinematic viscosity: $v := 15.69 \cdot 10^{-6} \cdot m^2 \cdot s^{-1}$

Prandtl number: $Pr := 0.708$

Thermal conductivity: $k := 0.02624 \cdot W \cdot m^{-1} \cdot K^{-1}$

The dimensions of the surfaces of the zones are typically 0.45x0.93 m. To calculate the Reynolds number a dimension of 0.93 m will be used.

The inside air was stirred by a small fan. The maximum air speed close to the fan was measured with a hot wire anemometer at 5 m/s. The flow speed at the surfaces was measured between .1 and .5 m/s.

Typical dimension: $x := \sqrt{0.45 \cdot 0.93 \cdot m}$

Index: $i := 0 \,..\, 10$

Free stream flow speed: $u_i := \frac{i}{10} \cdot m \cdot s^{-1}$

Reynolds number: $Re_i := u_i \cdot \frac{x}{v}$

Reynolds number

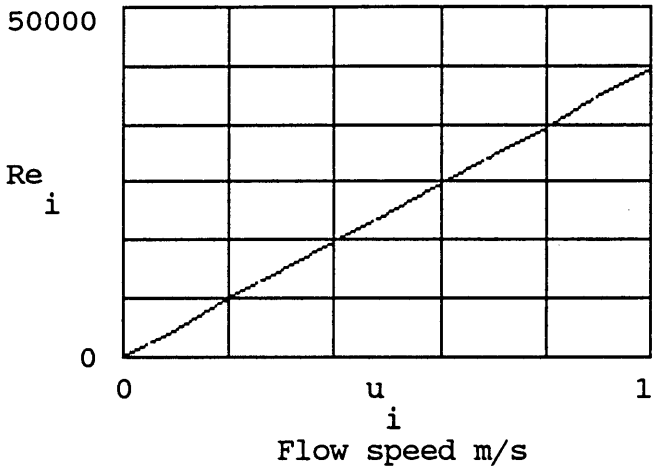

The Reynolds number is less than 500000 so it can be assumed the flow is reasonably laminar. Holman gives an equation for the mean Nusselt number accross the surface for these conditions.

$$\text{Nusselt number:} \quad Nu_i := 0.664 \cdot Re_i^{0.5} \cdot Pr^{0.333}$$

$$\text{Mean heat transfer coefficient:} \quad hm_i := Nu_i \cdot \frac{k}{x}$$

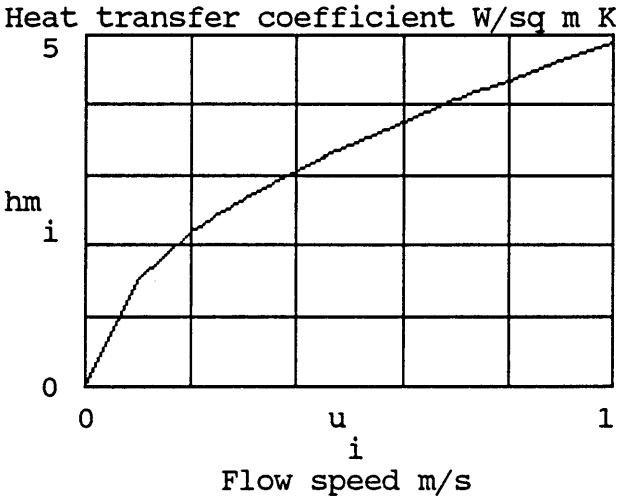

Flow speed

$$u = \begin{bmatrix} 0 \\ 0.1 \\ 0.2 \\ 0.3 \\ 0.4 \\ 0.5 \\ 0.6 \\ 0.7 \\ 0.8 \\ 0.9 \\ 1 \end{bmatrix} \cdot \frac{m}{s}$$

Reynolds

$$Re = \begin{bmatrix} 0 \\ 4123.109 \\ 8246.217 \\ 12369.326 \\ 16492.435 \\ 20615.544 \\ 24738.652 \\ 28861.761 \\ 32984.87 \\ 37107.979 \\ 41231.087 \end{bmatrix}$$

Coefficient

$$hm = \begin{bmatrix} 0 \\ 1.542 \\ 2.18 \\ 2.67 \\ 3.083 \\ 3.447 \\ 3.776 \\ 4.079 \\ 4.36 \\ 4.625 \\ 4.875 \end{bmatrix} \cdot W \cdot m^{-2} \cdot K^{-1}$$

According to this (probably naive) calculation the forced convection film coefficient is aproximately 3.5 W/sq m K.

Convection film coefficient: $hc := 3.5 \cdot W \cdot m^{-2} \cdot K^{-1}$

In the theoretical model the film heat transfer coefficient includes all contributions of heat flow from the surface of the partition to the air node. It is therefore neccessary to include flow contributions via radiation to the other walls and convection from these walls. This contribution is calculated by assuming the radiation causes no appreciable warming of the air. In this case the heat transfer coefficient for the other walls is found by adding the radiation resistance to the convection resistance, since no conduction takes place through the walls.

Estimate of Radiation Resistance

Stefan-Boltzman constant: $\sigma := 5.669 \cdot 10^{-8} \cdot W \cdot m^{-2} \cdot K^{-4}$

Shape factor: (For closed box) $F := 1$

Emmisivity for asbestos: $\epsilon := 0.96$ (Holman table A-10)

Mean Temperature: $T := 300 \cdot K$

Linearized radiative heat transfer coefficient:

$$hr := 4 \cdot F \cdot \sigma \cdot \epsilon \cdot T^3$$

$$hr = 5.878 \cdot W \cdot m^{-2} \cdot K^{-1}$$

Surface area of box walls excluding partition:

$$Ar := 3 \cdot 0.93 \cdot m \cdot 0.45 \cdot m + 2 \cdot 0.45 \cdot m \cdot 0.45 \cdot m$$

$$Ar = 1.661 \cdot m^2$$

Radiation resistance: $Rr := \frac{1}{Ar \cdot hr}$ $Rr = 0.102 \cdot K \cdot W^{-1}$

Convection resistance: $Rc := \frac{1}{Ar \cdot hc}$ $Rc = 0.172 \cdot K \cdot W^{-1}$

Partition surface area: $Ap := 0.45 \cdot m \cdot 0.93 \cdot m$

$$Ap = 0.419 \cdot m^2$$

Effective film coefficient referred to partition surface area:

$$he := \frac{1}{Ap \cdot (Rr + Rc)}$$

$$he = 8.704 \cdot W \cdot m^{-2} \cdot K^{-1}$$

Total partition surface heat transfer coefficient:

$$ht := hc + he$$

$$ht = 12.204 \cdot W \cdot m^{-2} \cdot K^{-1}$$

APPENDIX 4D

Verification of multi-zone solution for two zone model.

Define units: length mass time temperature

$m \equiv 1L \quad kg \equiv 1M \quad s \equiv 1T \quad C \equiv 1Q$

$J \equiv kg \cdot m^{2} \cdot s^{-2} \qquad W \equiv J \cdot s^{-1}$

$kJ \equiv J \cdot 10^{3} \qquad kW \equiv W \cdot 10^{3}$

$h \equiv 60 \cdot 60 \cdot s \qquad rad \equiv 1$

$deg \equiv \frac{\pi}{180} \cdot rad \qquad mm \equiv m \cdot 10^{-3}$

Resistance units: $\Omega \equiv C \cdot kW^{-1}$

Capacitance units: $F \equiv kJ \cdot C^{-1}$

Define frequency 1/24h:

$f \equiv 1 \cdot 24^{-1} \cdot h^{-1}$

$\omega \equiv 2 \cdot \pi \cdot f \qquad s \equiv i \cdot \omega$

Material parameters

The model is constructed of pressed asbestos cement with the following thermal characteristics.

$K := 0.62 \cdot W \cdot m^{-1} \cdot C^{-1}$ Thermal Conductivity

$\rho := 2100 \cdot kg \cdot m^{-3}$ Density

$\sigma := 0.83 \cdot kJ \cdot kg^{-1} \cdot C^{-1}$ Specific Heat Capacity

$l := 9 \cdot mm$ Thickness

During the experiment the sides and floor of the model were isolated from the environment with 40 mm thick polystyrene tiles. The roof was exposed. The dimensions of the enclosure are 450x450x930 mm. Note that a single asbestos cement layer of 9 mm formed the walls.

Area of non-isolated zone walls (roof): $An := 450 \cdot 930 \cdot mm^{2}$

$An = 0.419 \cdot m^{2}$

Total area of zone walls contributing to capacitance:

$$Az := (4\cdot(450\cdot 930) + 2\cdot(450\cdot 450))\cdot mm^2$$

$$Az = 2.079\cdot m^2$$

Since the outside of the model is exposed to the almost stationary air in the cellar. The convective heat and radiative heat transfer coefficients are estimated in appendix 4C. If the convective coefficient is taken as approximately 2 W/sq m K and the radiative as 5 W/sq m K the combined outside film coefficient is 5 W/sq m K. Allowing for another 5 W/sq m K for seepage of air through the cracks the total outside film coefficient is approximately 10 W/sq m K.

External film coefficient: $ho := 10\cdot W\cdot m^{-2}\cdot C^{-1}$

Shell resistance: $Ro := \left[\frac{1}{K} + \frac{1}{ho}\right]\cdot\frac{1}{An}$

$$Ro = 273.635\cdot\Omega$$

The inside air is stirred with a fan. In appendix 4C the interior film coefficient is crudely estimated at 12 W/sq m K.

Internal film coefficient: $hi := 12\cdot W\cdot m^{-2}\cdot C^{-1}$

$$Ra := \frac{1}{Az\cdot hi} \qquad Ra = 40.083\cdot\Omega$$

Heat storage capacitance: Asbestos - $Ca := \sigma\cdot\rho\cdot l\cdot Az$

Thermograph (3.3 kg Al) - $Cl := 3.3\cdot kg\cdot 0.88\cdot kJ\cdot kg^{-1}\cdot C^{-1}$

Total capacitance - $Ct := Ca + Cl \qquad Ct = 35.517\cdot F$

Thermal time constant: $\tau p := Ro\cdot Ct \qquad \tau p = 2.7\cdot h$

The calculated thermal time constant of 2.7 h agrees very well with the measured time constant of also approximately 2.7 h. It is therefore reasonable to assume that the capacitance and shell resistance values obtained above are not grossly in error.

The measured interior Thevenin temperature appears to be a perfect exponential charge and discharge with an amplitude of 9 degrees C and a time constant of 2.7 h. According to equation 3.1 in the text when Rv is infinite the theoretical Thevenin temperature for a 50 W step in the radiative source is:

$$Th(t) := 50\cdot W\cdot Ro\cdot\left[1 - e^{-\left[\frac{t}{\tau p}\right]}\right]$$

$i := 0 \,..31$ Hours index

$$Te_i := Th\left[i \cdot \frac{11}{31} \cdot h\right]$$

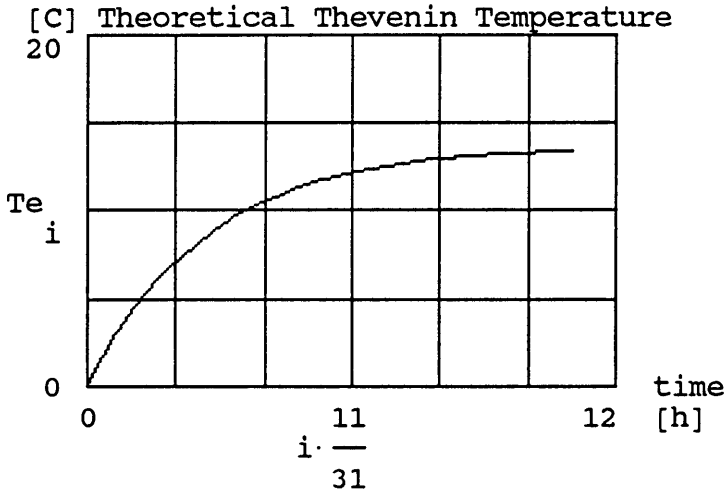

The calculated temperature swing is 14 degrees as opposed to the measured 9 degrees. Note however that we have taken all the heat dissipated by the lamp as radiative heat while, in practice, a fraction would be convective, which enters differently into the solution. Since the calculated time constant seems to agree with the measured time constant, it is suspected that the calculated Ro is fairly accurate unless the error in Ro is cancelled by an oposite error in the value of C. It seems the biggest uncertainties lie in the values of the film coefficients, but, notice that only the outside film coefficient plays a role in establishing the amplitude and time-constant in the absence of ventilation. From the discrepancy it appears probable that more infiltration took place than was accounted for in the outside film coefficient, or heat was lost to the outside through other paths.

Since we are interested in verifying the multi-zone model, and not so much the thermal properties of the construction materials we shall derive the value of the resistance Ro and capacitance C from the measured amplitude of the swing and time-constant.

$$Rom := \frac{9 \cdot C}{50 \cdot W} \qquad Rom = 180 \cdot \Omega$$

$$\tau m := 2.7 \cdot h$$

$$Cm := \frac{\tau m}{Rom} \qquad Cm = 54 \cdot F$$

Both the resistance and capacitance values differ significantly from the theoretical values. As discussed above the small experimental value of the resistance can be attributed to seepage of air but it is difficult to explain the extra heat capacitance. The density of the asbestos boards were measured and is in agree -ment with the value used above. The only conclusion we can come to is that either the specific heat capacitance value is underestimated or the isolation of the bottom from the concrete floor was ineffective. The latter effect would explain both the discrepancy in resistance and capacitance.

Fourier Analysis of experimental Thevenin temperature.

$$Tm(t) := 50 \cdot W \cdot Rom \cdot \left[1 - e^{-\left[\frac{t}{\tau m}\right]}\right]$$

$$Thm_i := Tm\left[\frac{11}{31} \cdot i \cdot h\right]$$

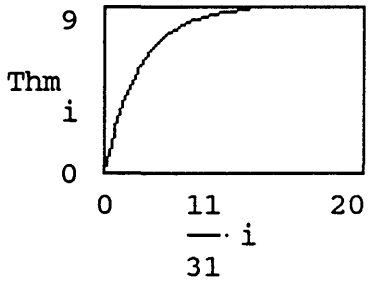

$Fr := fft(Thm)$

Frequency index"
$k := 0 \,..16$

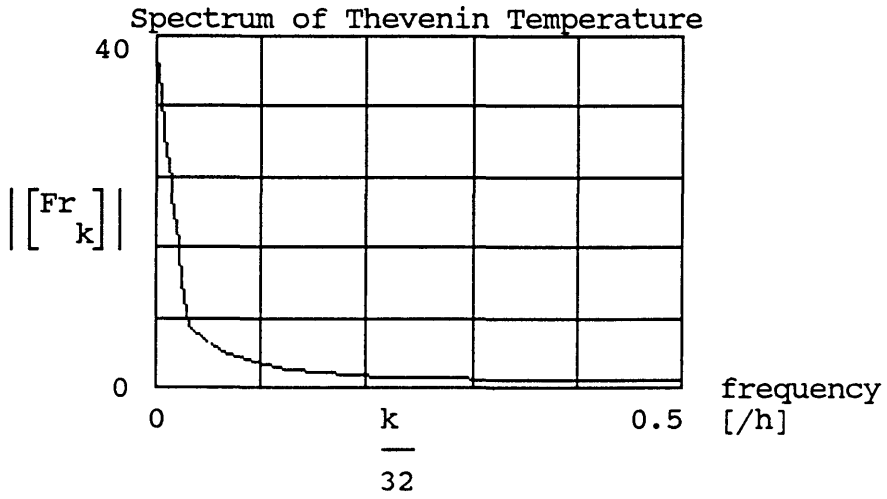

Source internal impedances:

$$Zi(s) := \left[\frac{Rom + Ra \cdot (\tau m \cdot s + 1)}{\tau m \cdot s + 1}\right] \qquad Zi(s) = 160.111 - 84.843i \cdot \Omega$$

Internal impedance matrix:

$$Z(s) := \begin{bmatrix} Zi(s) & 0\cdot\Omega \\ 0\cdot\Omega & Zi(s) \end{bmatrix}$$

Partition admittance matrix

Area of partition: $Ap := 930\cdot 450\cdot mm^2$ $\quad Ap = 0.419\cdot m^2$

Branch resistances (assuming one side exposed to heat source):

$$Rp := \begin{bmatrix} \frac{1}{K} + \frac{1}{hi} \end{bmatrix} \cdot \begin{bmatrix} \frac{1}{2\cdot Ap} \end{bmatrix} \qquad Rp = 116.905\cdot\Omega$$

Trunk capacitance:

$$Cp := \sigma\cdot\rho\cdot l\cdot Ap \qquad Cp = 6.565\cdot F$$

Partition admittance:

$$Y(s) := \frac{1}{Rp\cdot(Rp\cdot s\cdot Cp + 2)} \cdot \begin{bmatrix} Rp\cdot s\cdot Cp + 1 & -1 \\ -1 & Rp\cdot s\cdot Cp + 1 \end{bmatrix}$$

$$Y(s) = \begin{bmatrix} 0.004 + 1.193\cdot 10^{-4}\,i & -0.004 + 1.193\cdot 10^{-4}\,i \\ -0.004 + 1.193\cdot 10^{-4}\,i & 0.004 + 1.193\cdot 10^{-4}\,i \end{bmatrix}^{-1}\cdot\Omega$$

Multizone solution via matrix inversion:

$$I := \begin{bmatrix} 1 & 0 \\ 0 & 1 \end{bmatrix}$$

$$Hi(s) := (I + Z(s)\cdot Y(s))^{-1}$$

Interior temperature swings

Zone 1: $\quad Fi1_k := Hi\left[k\cdot 2\cdot\frac{\pi}{32\cdot h}\right]_{0,0}\cdot Fr_k$

Zone 2: $\quad Fi2_k := Hi\left[k\cdot 2\cdot\frac{\pi}{32\cdot h}\right]_{1,0}\cdot Fr_k$

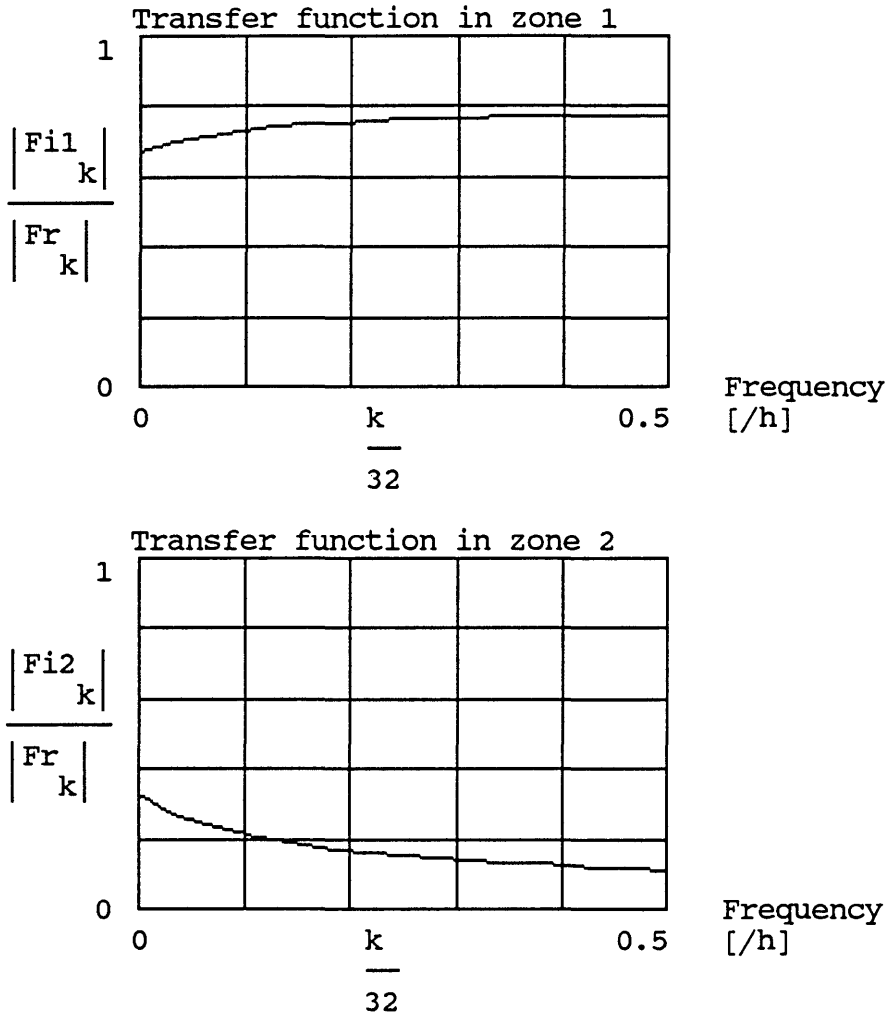

The graphs indicate the fraction of energy from the active zone which a) remains in the active zone and b) propagates to the inactive zone as a function of frequency. More energy is transferred at the lower frequencies because of the exponential decrease in temperature swing through the partition.

Time signals

Ti1 := ifft(Fi1) Ti2 := ifft(Fi2)

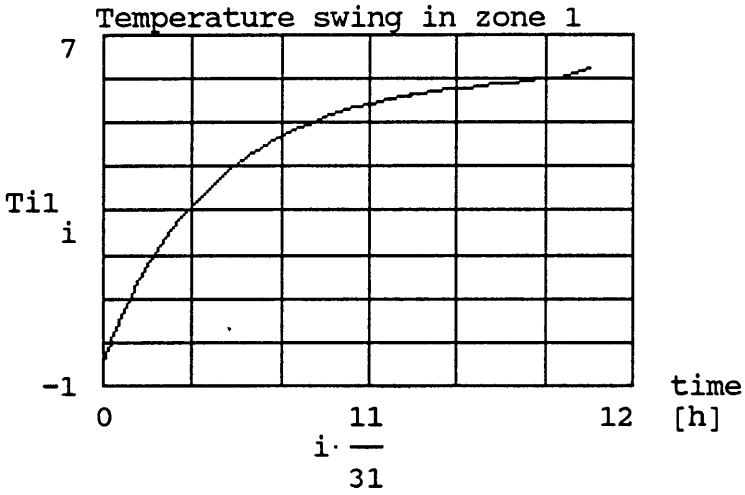

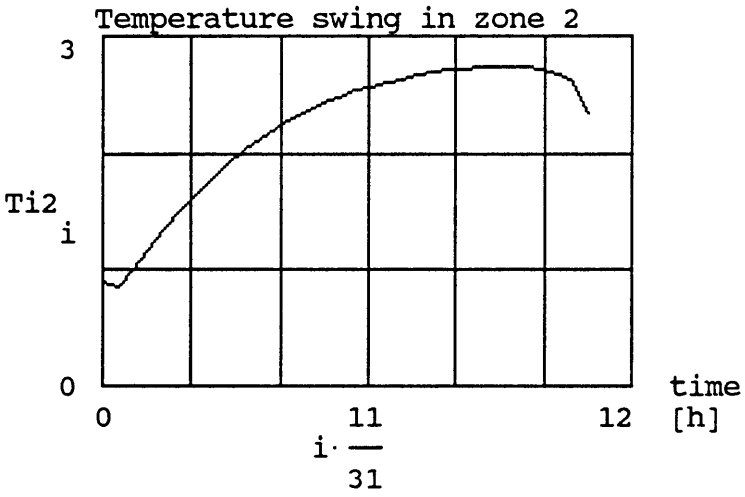

The calculated swings are 6 degrees in zone 1 and 2.7 degrees in zone 2. These values are very close to the measured swings in figure 4.8a and 4.8b of 6 and 3 degrees respectively.

Bearing in mind the difficulties experienced to obtain correct values for the surface heat transfer coefficients the measurements verify the theory.